Stony Brook University

The Pathogenic NY-1 Hantavirus Gn Cytoplasmic Tail Regulates Cellular Interferon Responses

A Dissertation Presented

by

Peter Joseph Alff

to

The Graduate School

In Partial Fulfillment of the

Requirements

for the Degree of

Doctor of Philosophy

in

Molecular and Cellular Biology

Stony Brook University

December 2007

Stony Brook University
The Graduate School

Peter Joseph Alff

We, the dissertation committee for the above candidate for the degree of Doctor of Philosophy, hereby recommend acceptance of this dissertation.

Erich R. Mackow – Dissertation Advisor
Professor – Department of Medicine

Nancy Reich – Chairperson of Defense
Professor – Department of Molecular Genetics and Microbiology

Patrick Hearing
Professor – Department of Molecular Genetics and Microbiology

James Bilska
Professor – Department of Molecular Genetics and Microbiology

This dissertation is accepted by the Graduate School.

Lawrence Martin
Dean of the Graduate School

Abstract of the Dissertation

The Pathogenic NY-1 Hantavirus Gn Cytoplasmic Tail Regulates Cellular Interferon Responses

by

Peter Joseph Alff

Doctor of Philosophy

in

Molecular and Cellular Biology

Stony Brook University

2007

Hantaviruses cause two diseases with vascular permeability defects, hemorrhagic fever with renal syndrome (HFRS) and hantavirus pulmonary syndrome (HPS). Non-pathogenic PHV elicits early interferon responses in human, suggesting that hantavirus pathogenesis may in part be determined by viral regulation of cellular interferon responses. In contrast to pathogenic NY-1V and HTNV, PHV replication is blocked in IFN competent human endothelial cells, further suggesting NY-1V might regulate early IFN responses. These findings led us to investigate the mechanism of interferon regulation by

pathogenic hantaviruses and what permits pathogenic hantavirus replication in human endothelial cells.

Expression of the NY-1V Gn cytoplasmic tail inhibited RIG-I and TBK1 directed transcription from interferon stimulated response elements (ISRE) or β-interferon promoters. In contrast, expression of the NY-1V nucleocapsid or PHV Gn-tail had no effect on RIG-I or TBK1 directed transcription. Further, neither the NY-1V nor PHV G1-tails inhibited transcriptional responses directed by a constitutively active IRF-3 protein. These findings indicate that the pathogenic NY-1V Gn protein regulates cellular IFN responses upstream of IRF-3 phosphorylation at the level of TBK1 signaling complexes.

TBK1 phosphorylates IRF-3, and forms a signaling complex with TRAF3, which is required for IFN transcription directed by a variety of upstream stimuli. TBK1 also forms a signaling complex with TRAF2, which directs NF-κB activation. Here we report that the NY-1V Gn-tail co-immunoprecipitates TRAF3, but not TBK1, from cellular lysates. Analysis of TRAF3 deletion mutants demonstrated that the Gn-tail bound the N-terminus of TRAF3, as well as the corresponding N-terminal domain of TRAF2. Furthermore, the NY-1V Gn-tail also inhibits TBK1 and TRAF2 directed NF-κB activation, indicating that the Gn-tail regulates the activation of two factors required for IFN-β transcription. In contrast, the Gn-tail of the non-pathogenic hantavirus PHV failed to bind TRAF3 or TRAF2 proteins or inhibit NF-κB or IFN-β transcriptional responses.

Expression of the NY-1V blocked TBK1 co-precipitation of TRAF3 and similarly, infection by NY-1V, but not PHV blocked the formation of TBK1-TRAF3 complexes. These findings suggest that both the NY-1V Gn-tail and infection by NY-1V virus disrupt the formation of TBK1-TRAF3 signaling complexes required for IFN-β induction.

Collectively, these findings indicate that the ability to inhibit interferon-β induction at early times post-infection is critical for hantavirus infection of human endothelial cells and suggest that the pathogenic hantavirus Gn cytoplasmic tail is the primary determinate of hantavirus pathogenic potential in humans.

Table of Contents

List of Tables

List of Illustrations

List of Figures

CHAPTER 1:

Introduction

Section 1: Hantaviruses

Historical Perspective

Hantavirus associated diseases were first described in Soviet and Japanese troops stationed in eastern Asia in the 1930s (48). Troops were afflicted with a hemorrhagic disease yet the causative agent and route of infection resulting in this affliction was unknown. Further study of this disease came in the early 1950s during the Korean War when over 3,000 UN troops developed a severe hemorrhagic disease characterized by acute thrombocytopenia (48). This syndrome was termed Korean Hemorrhagic Fever (KHF), however, it was not until 1973 that the causative virus was isolated from its small mammal host *Apodemus agragius*. The virus was given the name Hantaan virus, after the Hantaan River in Korea near which it was isolated (48). Throughout Asia, Hantaviruses remain a public health problem with the majority of infected individuals living in rural areas where they come in contact with rodents that harbor the virus.

Diseases similar to KHF, albeit with milder symptoms, were also documented throughout Europe and termed nephropathia epidemica (NE). We now know that NE is caused by a distinct hantavirus, Puumala Virus. Other KHF-like diseases were also documented in Finland and Scandanavia, as well as Russia. It became

apparent that many of the cases of KHF-like disease (now known as hemorrhagic fever with renal syndrome or HFRS) could be attributed to distinct hantaviruses. Interestingly, each of these viruses is carried by a specific small mammal host, which dictates their geographical location. One hantavirus, Seoul virus, is carried by rats and is thus believed to be a cause of HFRS worldwide.

Emergence of hantaviruses causing HPS

In 1993, an outbreak of an unknown severe respiratory disease occurred in the southwestern United States in the four-corners area (83). Patients presented with shortness of breath and suffered from an acute pulmonary edema, causing a form of acute respiratory distress syndrome (ARDS). Patients also exhibited acute thrombocytopenia (83). Most of these patients reported contact with rodents while harvesting pine nuts. Analysis of patient serum revealed an antibody response to hantavirus antigen suggesting that they suffered from a new form of hantavirus disease. This suspicion was confirmed and the disease was called hantavirus pulmonary syndrome (HPS). The prominent pulmonary symptoms in HPS patients, distinguishes HPS from European and Asian HFRS. Further, startlingly high initial mortality rates were observed in HPS (70-90%) compared to HFRS (0.1-5%) patients (83, 84).

The virus responsible for the 1993 outbreak was originally named four corners virus until it, along with a nearly identical hantavirus identified in

California (Convict Creek), was renamed Sin Nombre virus (SNV) in 1994. These viruses serve as prototype HPS causing hantaviruses. After the four corners outbreak, HPS began to be identified elsewhere in the Americas (16, 47, 48, 54) (46, 57, 88, 95, 112). A fatal case of HPS in New York State prompted a search for hantavirus in the white-footed mouse *Peromyscus leucopus,* a distinct but related animal to the hantavirus host *Peromyscus maniculatis* in the South Western United States. A new HPS causing hantavirus, serotypically distinct from SNV was subsequently identified in *Peromyscus leucopus* (23, 69, 70).

The incidence of HPS is significantly lower than HFRS, with approximately 1000 cases of HPS since its recognition in 1993. The mortality rate of HPS causing disease has decreased dramatically from near 90% in 1993 to 40-50% in 2006. This decrease in mortality is primarily due to a better understanding of how to support HPS patients during critical stages of the disease (83, 132).

Hantavirus Hosts

Hantaviruses belong to the *Bunyaviridae* family and are the only members of the family that are not transmitted by arthropod vectors. Unlike other bunyaviruses, hantaviruses persistently infect their respective small mammal hosts. Each hantavirus has co-evolved within a its specific host, and as a result host and hantavirus phylogenies are nearly identical. The relationship between hantaviruses and their hosts is not only important for the genetic evolution of each

hantavirus, but also defines the geographic prevalence of hantaviruses and hantavirus disease (48).

Hantaviruses infect their hosts persistently, but have no deleterious effects on the animal. In both hosts and humans, pulmonary endothelial cells are the primary site of hantavirus infection. How hantaviruses are persistently maintained in their hosts, and how hantaviruses negotiate host immune responses has remained unresolved. Persistent infection over extended periods of time maintains hantaviruses within host populations and allows for periodic spread to humans.

Although hantaviruses are enveloped, hantaviruses are exceptionally stable in dried forms, facilitating viral spread through dried urine and feces from infected animals. Humans are not hantavirus hosts, and infecting humans represents a dead-end for hantavirus spread. There is one reported case of person-to-person transmission of the Andes (AND) strain of hantavirus, but further person-to-person transmission of this or any other hantavirus has not been documented (18).

Hantavirus Pathogenesis

Hemorrhagic fever with renal syndrome (HFRS) is caused by hantaviruses found throughout Europe and Asia (Table 1). HFRS causing hantaviruses include the prototype Hantaan virus (HTNV) as well as Puumala (PUU) and Dobrava (DOB) hantaviruses. Hantavirus Pulmonary Syndrome (HPS) causing

hantaviruses have been identified throughout the Americas. These so-called "New World" hantaviruses include the prototypical Sin Nombre virus (SNV) as well as New York (NY-1), Black Creek Canal (BCC) and Andes (AND) viruses (53, 83).

Pathogenesis: Hantaviruse diseases are generally characterized by microvascular leakage, hemorrhage, and pulmonary edema (48). The primary site of infection in both HFRS and HPS patients is the pulmonary endothelium. However, the endothelium of other organs, including the heart, kidney, liver, and spleen is also infected. Hantavirus antigens (N-protein) can also be detected in other cell types including; circulating mononuclear cells, Kupffer cells, pulmonary macrophages and splenic dendritic cells. In HFRS patients, viral antigen can also be found in the pituitary and brain.

Clinical characteristics of HFRS: The onset of symptoms occurs approximately 2-3 weeks after infection with HFRS causing hantaviruses. The initial symptoms include high fever, chills, headache, myalgia and lumbar back pain (60). These nondescript "flu-like" symptoms lack one important component, cough, and make proper diagnosis difficult. The progression of HFRS has been separated into five stages (febrile, hypotensive, oliguric, diuretic, and convalescent) with the severity characterized as mild, moderate, or severe. Not every patient exhibits the same clinical course, further complicating diagnosis (10, 116). HFRS has a mortality rate ranging from 0.1-5% with the causes of death including; shock (75%), uremia (50%), pulmonary edema (15%) and central nervous system hemorrhage or

encephalopathy (5%). Full recovery from HFRS often takes 6 months to 1 year (48, 56).

Clinical Characteristics of HPS: Symptoms begin 2-3 weeks after infection, and are similar to HFRS (132). In the case of HPS however, initial "flu-like" symptoms develop into acute pulmonary edema, resulting in a viral form of acute respiratory distress syndrome (ARDS) (42). Leukocytosis with the occurrence of activated lymphocytes in peripheral blood has also been noted. HPS can be characterized by four distinct stages (febrile, cardiopulmonary, diuretic, and convalescent) and has a mortality rate of approximately 40%.

Common elements of HFRS and HPS: All hantaviruses predominately infect pulmonary endothelial cells, and common characteristics of both HFRS and HPS include increased vascular permeability, hemorrhage or edema, and acute thrombocytopenia (platelet loss). Either disease may also have pulmonary or renal components.

Treatment of hantavirus diseases: Currently there is no definitive treatment for HFRS or HPS. The antiviral drug Ribavirin has been used to treat some HFRS cases; however, Ribavirin has been shown to be effective only when administered early after infection. The effectiveness of Ribavirin in treating HPS is even less clear (72, 73). Interferon treatment is effective, but only if administered within 48 hours of infection (117, 118). After the onset of symptoms there is no effect of interferon on hantavirus disease, greatly limiting the usefulness of interferon as a

therapeutic agent. For both HFRS and HPS, treatment consists largely of supportive care, including fluid management, controlled electrolyte balance, and ventilation support. These measures have lead to the significant decrease in HPS case mortality rates between 1993 and 2006 (55).

Table 1

Name	Abbr.	Location	Disease
New York	NY-1	New York	HPS
Sin Nombre	SN	US, Canada	HPS
Black Creek Canal	BCC	US	HPS
El Moro Canyon	ELMC	S.W. United States	HPS
Andes	AND	S. America	HPS
Bayou	BAY	Louisiana	HPS
Puumala	PUU	Europe	HFRS
Seoul	SEO	Asia	HFRS
Hantaan	HTN	Asia	HFRS
Prospect Hill	PH	N. America	None
Tula	TUL	Europe	None

Hantavirus structure and genetics

Hantaviruses, like other bunyaviruses, are enveloped, negative-stranded RNA viruses (48, 102). The hantavirus genome consists of three RNA segments: small (S), medium (M), and large (L), each with conserved and complementary nucleotides on their ends. The size of the RNA segments vary considerably, with S segment ranging from 1.7-2.1 Kb, M segment being 3.6 Kb, and L segment being 6 Kb. The high degree of conservation between the complimentary end-terminal sequences of hantaviruses and other bunyaviruses suggest that these untranslated regions (UTRs) play a critical role in RNA replication and transcription. Hantavirus particles average 100 nm in diameter with a spherical shape and a highly structured, grid-like pattern on their surface formed by the viral surface glycoproteins. Hantaviruses encode only four structural proteins; the nucleocapsid (N-protein), Gn and Gc surface glycoproteins, and the viral polymerase (48, 102).

S segment encodes the nucleocapsid protein, the most abundantly produced viral protein during hantavirus infection and the major antigenic determinate of all hantaviruses. N-protein is detectable 6-12 hours post-infection and is highly expressed in infected cells. The role of N-protein in the hantavirus life cycle has been extensively studied and appears to be multifaceted. N-protein encapsidates the viral genomic RNA as well as cRNA intermediates (required to make mRNA) and remains complexed with RNAs during transcription and

replication. N-protein has been shown to form dimers and trimers, both by yeast and mammalian two-hybrid analysis. These N-protein dimers and trimers likely multimerize into even larger oligomeric structures and encapsidate viral RNA. N-protein also protects viral genomic RNA from degradation and is required for the proper assembly of virions.

M segment encodes a viral proprotein which is co-translationally cleaved after a conserved WAASA sequence into the N-terminal Gn and C-terminal Gc glycoproteins (67). Gn contains a predicted signal sequence, several transmembrane domains, a double hydrophobic anchor sequence, predicted RING and zinc-finger domains, and a 142 amino acid long cytoplasmic tail. Interestingly, the Gn cytoplasmic tail of pathogenic, but not non-pathogenic hantaviruses directs proteasomal degradation, suggesting that Gn degradation may play a role in hantavirus pathogenesis (26, 106).

Gc lacks a signal sequence, but is C-terminally anchored in the membrane and contains a short cytoplasmic tail with an eight-residue ER retention sequence. Gn and Gc proteins differ between hantaviruses, with approximately 40-60% identity at the amino acid level. Gn and Gc are glycosylated and HPS causing hantaviruses contain conserved cysteine residues, suggesting Gn and Gc structure is similar between these hantaviruses. The divergence of Gn and Gc primary amino acid sequence, however, results in antibody responses that are generally specific for a single hantavirus.

Similar to other members of the *Bunyaviridae* family, hantavirus maturation requires trafficking of the viral glycoproteins to endoplasmic reticulum (ER) and cis-Golgi compartments (79, 108, 110). When expressed individually, Gc is retained in the ER, while Gn appears to localize to the cis-Golgi. Co-expression of Gn and Gc traffics both proteins to the cis-Golgi, which is where hantavirus budding occurs. The precise Gn/Gc sequences that direct cis-Golgi trafficking and localization are currently unknown. Hantaviruses bud into the lumen of the cis-Golgi, and exit cells via a mechanism consistent with an aberrant secretory pathway (48). Although one report suggests that the Black Creek Canal hantavirus matures at the plasma membrane, Gn and Gc of BCC do not traffic to the plasma membrane indicating that this data may misinterpret the presence of cell-associated secreted virus (93).

The hantavirus L segment encodes the 220 KDa RNA dependent RNA polymerase (102). This protein shares sequence homology with other known viral polymerases. The amino acid homology between hantavirus L proteins is very high, reflecting evolutionary conservation of this viral gene product.

Hantavirus genomes are segmented, and thus have the potential to reassort gene segments during mixed infection. Interestingly, only a single M segment reassortant, between the highly homologous SNV and ANDV, have been recovered (and only in one direction) and reassortants between diverse hantaviruses have not been generated (36, 96, 97). These findings suggest that N-

protein and polymerases for each hantavirus have coevolved, and are tightly linked to successful hantavirus replication.

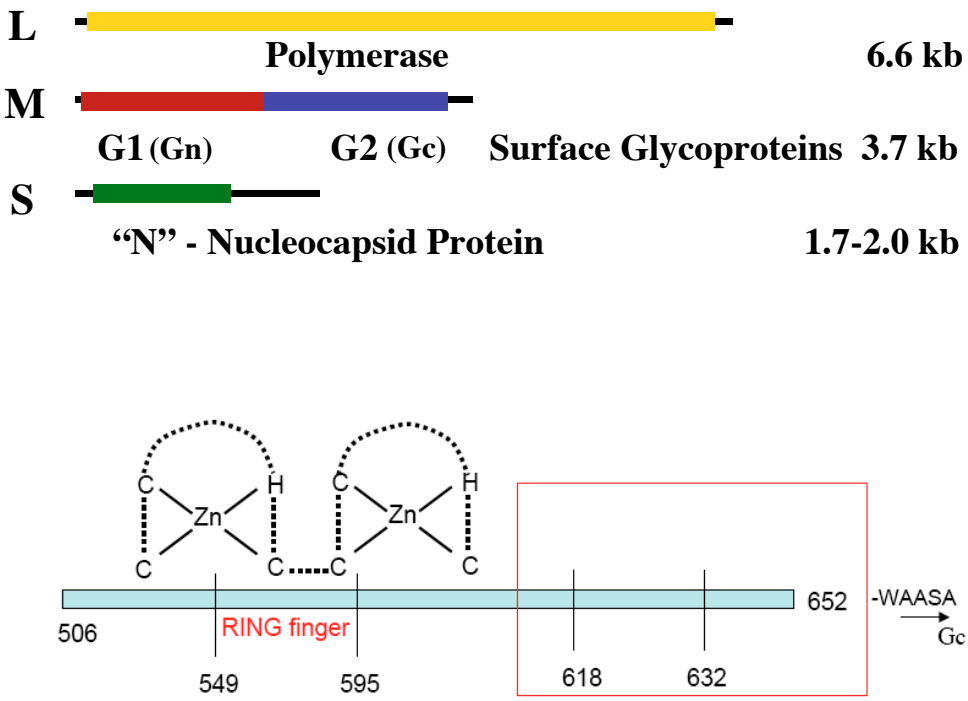

Schematic representation of the hantavirus genome and encoded proteins. The Gn cytoplasmic tail, showing RING finger domains, and WAASA cleavage site which separates Gn from Gc.

Section 2: Interferon Response

Cellular Recognition of Viral Infection

Innate cellular immune responses are a cell's first line of defense against viral infection, replication, and spread. Mammals have evolved a variety of cellular receptors which recognize viral infection, initiate signal transduction cascades, and ultimately direct the production of type-I interferons that elicit an antiviral state (51, 61, 100, 119). Type-I interferons are cytokines which include a single IFN-β and multiple IFN-α gene products that restrict viral infection (87, 124). Interferons are secreted and bind, in an autocrine and paracrine fashion, to cellular IFN receptors (IFNAR). Interferon receptors direct a cascade of signaling events, resulting in the expression of a large subset of interferon stimulated genes (ISGs), which restrict viral replication within the cell. However, in order for IFN to be induced, host cells must recognize viral infections and this initial recognition step is critical in mounting an effective antiviral response.

Viral particles and specific products of viral replication are recognized by host cells and are referred to collectively as pathogen associated molecular patterns or PAMPs (80, 85, 100). Cellular proteins that recognize and respond to virus infection are termed pattern recognition receptors (PRRs). The two main groups of these proteins are the Toll-like receptors (TLRs) and a family of RNA helicases, including retinoic acid-inducible gene I (RIG-I) and melanoma differentiation associated gene 5 (MDA5). These PRRs vary in their expression

between cell-types, and are specific for different aspects of viral infection. A common feature of PRRs is that they activate signaling cascades, which converge on the activation of the latent transcription factors IRF-3 and NF-κB that drive IFN gene transcription (87).

Toll-like Receptors: Toll-like receptors are expressed in a variety of cell types, and are integral membrane proteins. TLRs have an extracellular ligand binding domain and a cytoplasmic Toll/Il-1R homology (TIR) domain. Upon ligand binding, TLRs signal through cytoplasmic adaptor proteins TRIFF or MyD88 to direct IFN-β gene expression (76). There are 13 known TLRs, six of which (TLRs 2, 3, 4, 7, 8, and 9) have been shown to function in viral recognition. Some TLRs recognize viral protein components (TLR2 and TLR4), while others recognize viral RNA (TLR3, TLR7 and TLR8) and one (TLR9) recognizes viral DNA. TLR2 and 4 bind ligands on the cell surface, whereas TLR3 is associated with endosomes and recognizes viruses during endosome mediated endocytosis. Irrespective of ligand specificity or sub-cellular localization, TLR signaling activates IRF-3 and NF-κB resulting in IFN induction.

Cytoplasmic Recognition of Viral RNA: RIG-I and MDA5 have been shown to function as cytoplasmic sensors of virus infection in the cytoplasm (50, 131). These RNA helicases are unique among cellular helicases because they contain tandem caspase activation and recruitment domains (CARDs) (21). CARDs direct interactions with other CARD containing proteins, and function as cell-signaling

domains. Both RIG-I and MDA5 have been shown to bind synthetic RNA and *in vitro* transcribed RNA. Upon binding to viral RNA, RIG-I and MDA5 undergo a conformational change, resulting in the exposure of their CARDs, which interact with a mitochondrion associated adaptor protein, IPS-1/MAVS/Cardiff/VISA (52, 107, 128). This interaction directs the organization of a multimeric signaling complex containing TBK1, which directs NF-κB activation and IRF-3 phosphorylation (38).

TRAF3 Plays a Central Role In Interferon Signaling: TRAF3 has recently been shown to play an important role in signaling pathways leading to IFN-β induction (32, 77). TRAF3 binds to the TRAF interacting motif (TIM) within IPS-1 through its C-terminal TRAF domain (99). TRAF3 also binds TBK1, linking upstream viral recognition responses to TBK1 phosphorylation of IRF-3 and downstream transcriptional effector functions. IRF-3 phosphorylation likely requires the proper assembly of a macromolecular signaling complex consisting of IPS-1, TBK1, IRF-3 and TRAF3 (40, 41). Although the requirements of TBK1-TRAF3 binding have yet to be defined, studies in TRAF3 knockout cells revealed IRF-3 phosphorylation and IFN-β production in response to RIG-I and TLR signaling require TRAF3 (77).

Interferon-beta Induction

IRF-3 and NF-κB activation are required for IFN-β transcription. NF-κB activation requires IKK kinases, which phosphorylate the NF-κB inhibitor IκBα. IκBα phosphorylation results in IκBα degredation by the proteasome and release of NF-κB transcription factors, which translocate to the nucleus and activate transcription from the IFN-β promoter (39). TANK-binding kinase-1 (TBK1) simultaneously phosphorylates cytoplasmic IRF-3 at C-terminal serines, resulting in IRF-3 dimerization and nuclear translocation (31). In the nucleus, IRF-3 transcription factors bind DNA elements within the IFN-β promoter and in the context of NF-κB, basal transcription factors (CBP/p300) and AP-1 direct IFN-β transcription (11, 124).

Interferon receptors (IFNAR) dimerize in response to IFN binding, and activate receptor-associated Janus kinases (JAKs) (12, 121). JAKs phosphorylate signal transduction and activator of transcription (STAT) factors (STAT1 and STAT2), which associate with a third transcription factor, IRF9, and activate transcription from interferon stimulated response elements (ISRE) (86, 134). The result is the production of many ISGs that inhibit viral transcription and replication. Among the most studied ISGs are myxovirus resistance gene A (MxA) and 2'-5' oligoadenylate synthases (OAS). MxA is a GTPase which exerts its antiviral effects by sequestering viral ribonucleoproteins. OAS activation results in 2'-5' oligoadenlyates and the activation of ribonuclease L (RnaseL)

which degrades viral RNA (22). There are many other less well characterized ISGs many of which have unknown functions. The diversity of ISGs, and the antiviral properties of these proteins suggest that hosts have evolved mechanisms to cope with a variety of viral infections through the common induction of innate immune responses. Viruses on the other hand have likewise evolved a wide array of mechanisms for evading host cell defense mechanisms and to successfully replicate within cells.

Section 3:

Viral Strategies for Regulating Interferon

Viral replication requires the successful negotiation and regulation of innate cellular responses, and many viruses block signaling pathways that direct IFN transcription in order to bypass cellular regulatory mechanisms. A virus's ability to negotiate early interferon responses often differentiates pathogenic from non-pathogenic viruses. Viruses have evolved mechanisms to evade immune surveillance, block acquired immunity, neutralize the effects of anti-viral cellular proteins, and inhibit cellular interferon signaling pathways. The variety of receptors and pathways involved in recognizing viruses and activating interferon signaling responses provide many possible targets for viral to regulation.

The hepatitis C virus NS3/4A protein cleaves IPS-1 at a defined cysteine residue dissasociating IPS-1 from the mitochondria. By cleaving and altering the sub-cellular localization of IPS-1, hepatitis C prevents IRF-3 phosphorylation, NF-κB activation, and IFN-β production, allowing the virus to replicate successfully (17, 62, 64, 74). The Ebola virus (EBOV) VP35 protein also blocks the virus-induced phosphorylation and activation of IRF-3 by binding dsRNA but also appears to block IPS-1 and TBK1 directed transcriptional responses in a dsRNA binding independent manner (7, 13). The rotavirus NSP-1 protein reportedly prevents IRF-3 phosphorylation by inducing the proteasomal

degradation of IRF-3 and may also bind dsRNA (5, 29). The influenza virus NS1 protein is also an IFN antagonist with reported dsRNA binding activity. NS1 has also recently been shown to inhibit IFN-β gene expression through binding interactions with RIG-I and IPS-1 (30, 58, 75, 78).

Some viruses target later steps in IFN signaling. Poxviruses produce a soluble homologue of the interferon receptor (IFNAR), which competes for secreted IFN, preventing it from binding the cellular IFNAR (2, 115). Paramyxoviruses V and W proteins bind STATs, and block JAK/STAT signaling, in some cases targeting STATs for proteasomal degradation. Some viruses target ISGs themselves while others, including herpesviruses induce cellular suppressors of cytokine signaling (SOCS), which inhibit ISGs. With host immune responses being so diverse, it is not surprising that viruses have evolved mechanisms that oppose cellular recognition strategies which activate the interferon system.

Hantaviruses and Interferon

Hantaviruses must also regulate interferon in order to successfully replicate in human cells. Hantaviruses have 3 cytoplasmic proteins, the polymerase, nucleocapsid protein and Gn cytoplasmic tail, that have the potential to regulate innate cellular responses (105, 111). The hantavirus Gn protein contains a large 142 residue cytoplasmic tail which reportedly binds cellular kinases and is ubiquitinated and degraded by the proteasome (26, 27). However, a

role for Gn-tail interactions in the regulation of cellular IFN responses has not been established.

The ability of hantaviruses to enter endothelial cells and establish persistence in animals suggests that all hantaviruses are able to regulate innate endothelial cell defenses within their hosts. The dramatic induction of IFN responses by PHV, but not pathogenic NY-1V (HPS) or HTNV (HFRS), 1 day post-infection of human endothelial cells suggested that differences in hantavirus directed interferon responses might determine the pathogenic potential of hantaviruses at a post-entry step (Table 2) (28, 59).

Table 2

Interferon Stimulated gene	HTNV	NY-1V	PHV
IFN inducible protein 9-27			229
MxA		3.7	161
IFN inducible 56kDa protein (ISG56)		2.8	154
CIG49			83
2-5" oligo A synthetase E gene			55
2-5" oligo A synthetase 59 kDa isoform			50
IFP35			42
IFN-inducible peptide(6-16)		2	41
CIG5			37
1.6 Kb mRNA for 2-5A synthatase			31
HEM45			19
Nuclear Phosphoprotein IFN induced			18
MxB			16
69 kDa 2-5" oligoadenylate (71kDa)			15
IFN induced 17-kDa/15-kDa protein			13
Hepatitis C assoc. microtub agg. protein p44			13
ISG 54-K			12
IFN regulatory factor (IRF) 7B			12
ISGF-3			9.3
p27			6.3
GBP2			6.3
Retinoic acid- and IFN-inducible 58K prot. RI58			5.4
Ly-6-related protein (9804)			4.1
Staf50			3.8

Differential Regulation of Endothelial Cell Interferon Responses 1 Day Post-infection.

RNA was extracted from cells from cells 24 h p.i. The Human Genome HGU95Av2 GeneChip (Affymetrix), containing 12,000 known genes, was hybridized, washed, and scanned according to Affymetrix protocols. Changes in cellular mRNA levels after hantavirus infection were compared with mRNA levels in mock-infected controls that were identically plated, treated, and incubated in the absence of virus. Affymetrix Micro Array Analysis Suite, Version 4.0.1, was used to normalize and scale results and compare viral responses to those of controls. Data represents fold-change relative to mock-infected control. (28)

Chapter 2:

Experimental Procedures

Cells and Virus

Biosafety level 3 (BSL-3) facilities were used throughout these experiments for hantavirus cultivation. Vero E6 cells were grown in Dulbecco's MEM (DMEM), 10% fetal calf serum (FCS), L-glutamine, penicillin, and streptomycin (GIBCO). Human umbilical vein endothelial cells (HUVECs) were purchased from Clonetics (Walkersville, MD). Endothelial cells were grown in endothelial cell basal medium-2 (EBM-2) supplemented with human recombinant epidermal growth factor (10 ng/ml), hydrocortisone (1μg/ml), gentamicin (50 μg/ml), amphotericin B (50 μg/ml), 0.1% endothelial growth factor, and 2% FCS (Clonetics) (25). HUVECs were used for 3-6 passages. New York-1 (NY-1V), Hantaan 76-118 (HTNV) and Prospect Hill (PHV) viruses were mycoplasma free and cultivated in Vero E6 cells (103).

Hantavirus Infection

Cells were infected in 6-well plates with viral stocks containing approximately 5 x 10^5 Focus Forming Units (FFU) per ml as determined by focus assay on Vero E6 cells (25). Virus was adsorbed to cells at a multiplicity of infection (MOI) of 1 for 1 hour at 37° C as indicated. Virus was removed, monolayers were washed with media and cells were maintained in complete media with 2% FCS. At various times post infection (p.i.) the titer of virus in cell supernatants was determined by titration on Vero E6 cells. In some experiments

1000 IU/ml human IFN-α (Sigma) was added 24 h prior to, or at various times after, mock infection or infection with NY-1, HTN, and PH viruses (MOI of 1). In other experiments cells were treated with 500 U/ml of neutralizing antibody to IFN-α or IFN-βas indicated following adsorption. These experiments were performed at least five times with similar results.

Immunoperoxidase Staining of Hantavirus Infected Cells

Immunoperoxidase staining of the hantavirus nucleocapsid protein within infected cells was performed as follows. Cell monolayers were fixed with 100% methanol and incubated with a rabbit polyclonal anti-nucleocapsid serum (1:2000) made to the recombinant nucleocapsid protein of NY-1V. Monolayers were washed with PBS and incubated with goat anti-rabbit horse-radish-peroxidase (HRP) conjugate (Kirkegaarde and Perry Laboratories). Monolayers were washed with PBS and stained with 3-amino-9-ethylcarbazole (0.026%) in 0.1 M sodium acetate, pH 5.2 and 0.03% H_2O_2 for 5-30 minutes (23). Monolayers were washed with distilled water and the number of nucleocapsid protein containing infected cells present in duplicate wells was quantified and compared to controls.

Bacterial Transformation

XL1 blue competent cells were transformed by electroporation and

prepared as follows. Cells were grown overnight and diluted 1:50 in 1000 ml of fresh Luria broth (LB; 1% NaCl-1% tryptone-0.5% yeast extract, pH 7.0) and grown at 37°C to an A_{600nm} of 0.6. Cells were pelleted in a Sorvall Superspeed centrifuge at 5000 rpm for 5 min and pellets were washed in ice-cold sterile water. Cells were subsequently washed in 10 % ice-cold glycerol, aliquoted 50 μl per 1.5 ml tube (again in 10 % glycerol), and flash-frozen in a dry ice/ethanol bath. Cells were stored at -80°C until use.

For transformation, frozen XL1 blue competent cells were thawed on ice, 1-2 μl (~0.1-10 ng) DNA was added, and cells were transferred to a pre-chilled 0.1 ml cuvette (Invitrogen). Cells were electroporated using a Bio-Rad gene pulsar (200 ohms, 25 μF, 1.25 kV). One ml of pre-warmed (37°C) LB was immediately added to cells, which were incubated for recovery at 37°C for 1 hour with shaking. To obtain bacterial colonies containing the plasmid of interest, transformed cells were plated to LB agar plates with the appropriate antibiotic(s), and incubated at 37°C overnight.

Preparation of Plasmid DNA

Alkaline Lysis Mini-prep: A 2 ml LB culture was grown overnight at 37°C with shaking. Cells were pelleted at 5000 X g for 5 min and resuspended in 100 μl Solution I (50 mM glucose, 25 mM Tris pH 8.0, 10 mM EDTA, + RNase A). Cells were lysed in Solution II (200 mM NaOH, 1% SDS) at room temperature

for 1 min and subsequently neutralized with 160 μl Solution III (3 M potassium, 5 M acteate) to precipitate protein and genomic DNA. The prep was centrifuged at 13,000 X g for 18 min at room temperature. The cleared lysate was moved to a clean tube. An equal volume of room temperature isopropanol was added to the lysate and mixed gently to precipitated plasmid DNA, which was pelleted by centrifugation at 13,000 X g for 14 min. The resulting supernatant was discarded and the pellet was washed with 70% cold ethanol and resuspended in 50 μl TE (25 mM Tris, 10 mM EDTA, pH 8.0) or distilled water.

Alkaline lysis maxi-prep: A 500 ml LB culture was grown overnight at 37°C with shaking. Cells were pelleted at 5000 X g for 5 min and resuspended in 10 ml Solution I + RNase A. Cells were lysed in 10 ml Solution II (200 mM NaOH, 1% SDS) at room temperature for 5 min and subsequently neutralized with 10 ml Solution III (3 M potassium, 5 M acteate) on ice for 20 minutes to precipitate protein and genomic DNA. The prep was centrifuged at 10,000 X g for 30 min at 4°C. The cleared lysate was added to a plasmid DNA purification column (Qiagen). Column-bound DNA was washed twice with 70% ethanol and eluted in a high-salt Tris (pH 8.0) buffer. Eluted DNA was precipitated by adding 0.7 X volume of isopropanol and precipitated DNA was pelleted by centrifugation (10,000 X g for 45 min at 4°C). Pellets were washed with 70% ethanol, resuspended in 500 ml TE (pH 8.0) and concentrations were determined by spectrophotometer.

Quantitative (Real-time) PCR analysis.

RNA Extraction: Total RNA was extracted from cells using the RNeasy kit (Qiagen, Chatsworth CA). Two confluent wells of HUVEC in 6-well plates were washed twice with PBS and lysed in a guanidine based lysis buffer (Buffer RLT with beta-mercaptoethanol). Lysates were purified using a silica-based column purification system (Qiagen) and column-bound RNA was washed with 70% ethanol and RPE buffer (Qiagen). RNA was eluted on ice with 35 μl RNase free water and concentration was determined using a spectrometer.

Generation of cDNA: RNA (1 μg) was reverse transcribed using oligo-$p(dT)_{15}$ or $p(dN)_6$ primers and the 1st Strand cDNA Synthesis Kit (Roche) according to the company's protocol. Primers were designed using Vector NTI Suite so that primer pairs were 100-150 nucleotides apart and had similar GC content and melting temperatures.

Primers: Specific primers were made to S segments from NY-1V, HTNV and PHV as well as GAPDH and MxA at nucleotide positions: NY-1V, forward 126-145; reverse 257-277 (109). HTNV, forward 798-817; reverse 914-933 (104). PHV, forward 184-203; reverse 307-326 (89). GAPDH forward 4357-4375 GGAAGCTCACTGGCATGGC; reverse 4408-4427 TAGACGGCAGGTCAGGTCCA (71). MxA, forward 379-397 TGATCCAGCTGCTGCATCCC; reverse 477-496

GGCGCACCTTCTCCTCATAC (1). Real-time PCR was performed with cDNA templates in Light Cycler reaction mix: FastStart DNA Master SYBR Green I (Roche), 4 mM $MgCl_2$, and 0.5 μM of each primer pair. Light Cycler PCR conditions were as follows: 95°C for 5 minutes followed by 30 cycles of: 95°C for 15 seconds, 62°C for 5 seconds and 72°C for 5 seconds amplification. Melting curve analysis was used to confirm PCR product identity. Results were compared to controls lacking cDNA template and GAPDH primer directed RT-PCR reactions were used to normalize sample cDNA levels (28). Experiments were performed three times with similar results.

For ISG56 analysis, HUVECs were infected with PHV or NY-1V and RNA was extracted as described above. ISG56 mRNA levels were determined relative to mock infected controls using TaqMan® primers for ISG56 (Applied Biosystems). Real-time PCR was performed using Applied Biosystems 7300 real time PCR machine. Thermo-cycling conditions were as follows: 50° C for 2 min, 95° for 10 min, 95° for 15 sec, and 60° for 1 min for a total of 40 cycles. All reactions were normalized to TaqMan® derived GAPDH mRNA levels.

Western Blot Analysis

N-Protein expression: HUVECs (1 X 10^5) were lysed in 250 μl Brugge buffer (0.5 % NP40) at various times p.i, protein levels were determined by BCA assay (Pierce) and 2.5-5 μg of protein were separated by 10% SDS-PAGE. Proteins

were transferred in a cold Tris-Glycine transfer buffer (30 % methanol) to nitrocellulose using a Novex Xcell electroblotter for 1 hour at 100V, blocked with 5% BSA and nucleocapsid proteins were detected using rabbit anti-nucleocapsid sera (1:10,000) followed by anti-rabbit HRP-conjugated antibody (1:5000) (Amersham) (Figure 3).

Gn-tail Gn cytoplasmic tail expression: NY-1V and PHV Gn-tail expression was evaluated following transfection of COS7 (Figure 10) or HEK 293 cells (Figures 13-16) that were treated with MG132 (50μM) 40 h post-transfection. Cells were lysed in 2X sample buffer (100 mM Tris-Cl pH 6.8, 200 mM DTT, 4% SDS, 0.2% bromophenol blue, 20% glycerol) and subjected to Western blot analysis 48 h post-transfection as described above using a monoclonal anti-GAL4 antibody (1:2000) from Santa Cruz Biotechnology (GAL4 [RK5C1], sc-510). Tubulin was detected using a monoclonal anti-tubulin antibody (1:2000) from Sigma (anti-β Tubulin clone TUB 2.1, T-4026) and Western Blots were developed using ECL reagent (Amersham) and exposure of blots to XAR-5 film (Kodak).

TRAF3 and TBK1 expression: TRAF3 and TBK1 expression was evaluated following co-transfection of HEK 293 cells treated with MG132 (50 mM) or the MG132 diluent, DMSO, by Western blot as previously described (106). Cells were lysed in 2X Laemmli sample buffer and analyzed by Western blot 48 hours post-transfection using anti-GAL4 (Gn-tail) (1:2000) or anti-*myc* (TBK1) (1:1000). Blots were washed with 1X Tris-buffered saline (TBS-T; 100 mM

NaCl, pH 7.4, 0.1% Tween 20) and incubated with HRP-conjugated anti-mouse IgG (1:3000). Western Blots were developed by fluorography in the presence of ECL reagent (Amersham). All Western blots were performed at least three times with similar results.

Protein Expression Plasmids and Transfections

Constructs expressing the NY-1V Gn cytoplasmic tail (pBIND-NY1G1cyto), PHV Gn cytoplasmic tail (pBIND-PHVG1cyto), and the NY-1V nucleocapsid protein (pBIND-NY1-S) were generated by C-terminally fusing coding regions to a GAL4 tag in the pBIND vector (Promega) (106). Coding regions were amplified with PCR primers containing *BamH*I and *Xba*I restriction sites and ligated directionally into the pBIND expression vector (Promega). All transfections were performed in sub-confluent monolayers of HEK 293 cells (~1 X 10^6) in 6-well plates (Corning, Inc) using the calcium phosphate method as previously described (26). pRK-FLAG-TRAF2 and pRK-FLAG-TRAF3 expression vectors have been previously described (98). Plasmids expressing TRAF2 and TRAF3 truncations (pRK-T3 N415 and pRK-T2 N355) were generated by inserting stop codons at amino acid positions 415 in TRAF3 and 355 in TRAF2 using a Quick-change sited directed mutagenesis kit (Stratagene). The pC-TBK1 expression vector has been previously described (90).

Site-directed Mutagenesis

The QuickChange site-directed mutagenesis kit was used for TRAF2 and TRAF3 mutagenesis reactions. Reactions contained; 10 mM KCl, 10 mM $(NH_4)_2SO_4$, 20 mM Tris-Hcl (pH 8.8) 2 mM $MgSO_4$, 0.1% Triton X-100, 0.1 mg/ml BSA, 50 ng DNA, 125 ng forward and reverse primers, 1µl *Pfu Turbo* DNA polymerase (elongation rate ~1 Kb/min). Amplification took place under the following thermocycling conditions:

95°C (30 seconds), 1 cycle

95°C (30 seconds), 55°C (1 min), 68°C (1-3 min), 16-18 cycles

4°C, hold.

After cycling was completed, 1 µl *DpnI* was added to each reaction and incubated at 37°C for 1-2 h to digest template plasmid. 1 ml of each reaction was transformed into chemically competent XL-1 gold cells by incubation on ice (30 min) and heat-shock (42°C, 45 seconds). Following heat-shock, 1 ml of warm LB was added to cells, which were incubated at 37°C for 1 hour with shaking for recovery.

Luciferase Assays

HEK 293 cells were co-transfected with 0.5 µg pISRE-Luc (Clontech Laboratories, Inc.) containing 5 copies of the ISRE binding site (5'

GATCCTCGGGAAAGGGAAACCGAAACTGAAGCC 3'), 0.5 μg of the IFN-β promoter luciferase reporter as indicated, as well as 250 ng of pRL (Promega), a constitutively active *Renilla* luciferase expression vector. Cells were co-transfected with 250-500 ng of a plasmid expressing myc-tagged TBK1 (pC-TBK1) generously provided by Dr. Joel Pomerantz and Dr. David Baltimore (*California Institute of Technology, Pasadena CA*) (90), or indicated amounts of a construct expressing N-terminal CARD domains of RIG-I (residues 1-284, (N)RIG; a gift from Dr. Michael Gale; *University of Texas Southwest Medical Center, Dallas TX*) (113) or a constitutively active form of IRF-3 (IRF-3 5D) (63) with an N-terminal GFP tag; a gift from Dr. John Hiscott, *McGill University, Montreal Canada*. Cells were transfected with indicated amounts of expression vector, and the total amount of plasmid DNA transfected was kept constant using empty pBIND vector. Cells were lysed 48 h post-transfection in 1X Passive Lysis Buffer (Promega) by incubation at 25°C (15 min) with gentle agitation. All luciferase assays were performed at least 3 times with similar results using the Dual Luciferase Assay System (Promega) and a Turner Designs TD 20/20 luminometer.

Transfection and hantavirus infection

Vero E6 Cells were transfected with TBK1 and TRAF3 expression vectors using Fugene HD (Invitrogen) in 6-well plates. Virus was adsorbed to cells 48

hours post-transfection at a multiplicity of infection of 1 for 1 hour at 37° C. Cells were washed and maintained in DMEM with 2% FCS. Two days post-infection cells were lysed in 200 µl of co-immunoprecipitation lysis buffer (20 mM Hepes pH 7.45, 75 mM KCl, 1.5 mM MgCl, 0.5 mM EDTA, 0.1% NP40, 1mM PMSF, leupeptin 10 μg/ml, aprotinin 10 μg/ml, pepstatin A 1 μg/ml, orthovanadate 1 μM, Na-pyrophosphate 5 μM, Na-F 1 μM) per well of a 6-well plate (32). Lysates were clarified by centrifugation (30 min at >10,000 x g) and TBK1 was immunoprecipitated with an anti-*myc* mAb. Protein A/G plus agarose beads (Santa Cruz Biotechnology) were added and immunoprecipitated proteins were analyzed as indicated.

Antibodies

Monoclonal anti-GAL4 antibody (GAL4 [RK5C1], sc-510) was purchased from Santa Cruz Biotechnology and monoclonal anti-FLAG M2 (F3165) antibody and monoclonal anti-β Tubulin (T4026) were purchased from Sigma-Aldrich. Anti-*myc* monoclonal antibody (R950-25) was purchased from Invitrogen. Anti-nucleocapsid rabbit polyclonal serum directed at the NY-1V nucleocapsid protein was used to detect N-protein form both NY-1V and PHV (26, 27). HRP-conjugated anti-mouse and anti-rabbit IgG secondary antibodies were purchased from Amersham Biosciences.

Transfections

Calcium Phosphate ($CaPO_4$): The following describes the $CaPO_4$ transfection method used per well of a 6-well plate (Corning, Inc). Up to 5 μg plasmid DNA was added to 148 μl distilled water at room-temperature along with 49.2 μl 2M $CaCl_2$ for a total volume of 200 μl. $CaCl_2$ was added to water and DNA 1 min prior to mixture with 200 μl 2X HBS (50 mM HEPES, 280 mM NaCl, 1.5 mM Na_2HPO_4). $CaCl_2$-DNA solution was added drop wise, over the course of 1 min, to the 2X HBS. Mixtures were incubated at room temperature for 5 min to allow formation of $CaPO_4$-DNA precipitates. Precipitates were added to HEK 293 cells (~70 % confluent) and incubated for 6-12 h at 37 °C. After transfection, cells were washed once with sterile PBS and grown in DMEM until analysis.

Fugene6 and Lipofectamine 2000: Fugene6 and LF2000 transfections were performed in monolayers of HEK 293 or COS7 cells (~75-95% confluent) in 6-well plates (Corning, Inc) using Fugene6 transfection reagent (Roche) or LF2000 (Invitrogen) according to manufactures instructions. Briefly, cells grown in one well of a 6-well plate were transfected using a 2:1 ratio (v/w) of Fugene6 or LF2000 to plasmid DNA. One μg of each plasmid was transfected per well as indicated for 16 h, washed with 1X PBS, and grown in complete DMEM (10% FCS, penicillin and streptomycin) for 48 hours prior to analysis.

Immunoprecipitation Assays

HEK 293 cells were transfected with plasmids expressing Gn-tail, TRAF3, TRAF2, or TBK1. Two days post-transfection, cells were washed with 1X PBS and lysed in co-immunoprecipitation lysis buffer as previously described. MG132 (50 μM) was added 6 hours prior to cell lysis unless otherwise indicated. Lysates were clarified by centrifugation and Gn-tail or TBK1 proteins were immunoprecipitated with anti-GAL4 or anti-*myc* mAbs, respectively, and protein A/G-plus agarose beads. Co-precipitated proteins were analyzed by Western blot as indicated.

Statistics

For replication, quantitative PCR, and luciferase assays, results are reported as ±SD for each group. For luciferase assays, a single-factor analysis of variance (ANOVA) was used to analyzes statistical differences between TBK1 activated control samples and samples expressing TBK1 and the NY-1V Gn cytoplasmic tail. Differences were considered statistically significant at $P < 0.05$. Below is a representative statistical analysis from figure 9.

Anova: Single Factor

SUMMARY

Groups	*Count*	*Sum*	*Average*	*Variance*
TBKI	2	56.7	28.35	0.605
NY-1V Gn-tail (0.5 μg)	2	42.6	21.3	0.72

ANOVA

Source of Variation	*SS*	*df*	*MS*	*F*	*P-value **	*F crit*
Between Groups	49.7025	1	49.7025	75.023	0.01306859	18.5128205
Within Groups	1.325	2	0.6625			
Total	51.0275	3				

SUMMARY

Groups	*Count*	*Sum*	*Average*	*Variance*
TBKI	2	56.7	28.35	0.605
NY-1V Gn-tail (0.4 μg)	2	3.6	1.8	0.18

ANOVA

Source of Variation	*SS*	*df*	*MS*	*F*	*P-value ***	*F crit*
Between Groups	704.903	1	704.903	1795.9	0.00055635	18.5128205
Within Groups	0.785	2	0.3925			
Total	705.688	3				

CHAPTER 3:

RESULTS

PHV Replication is Inhibited in Endothelial Cells

Pathogenic and non-pathogenic hantaviruses reportedly infect human endothelial cells (130). However, findings suggest that fundamental differences in hantavirus elicited interferon responses might limit replication of some non-pathogenic hantaviruses (28). Vero E6 cells which are used for the growth of all hantaviruses lack the type-I interferon locus, further suggesting that interferon responses of endothelial cells may restrict replication of some hantaviruses (15). Since there is little information on the replication of non-pathogenic hantaviruses in human endothelial cells, we compared the ability of non-pathogenic (PHV) and pathogenic hantaviruses (HTNV, NY-1V) to replicate in Vero E6 cells and HUVECs. Cells were infected at an MOI of 1 and virus present in cell supernatants was titered at various times post-infection (Figure 1A). PHV, NY-1V and HTNV replicated in Vero E6 cells resulting in titers of 1×10^3 to 1×10^4 FFUs/ml 3-4 days p.i. and reaching higher titers 6 – 7 days p.i. (Figure 1A). NY-1V and HTNV similarly reached titers of 1×10^3 to 1×10^4 FFUs/ml, 3-4 days post-infection of HUVECs (Figure 1B). In contrast, there was little PHV replication within HUVECs 1-7 days post infection, with maximal titers of 5-50 FFUs/ml in supernatants (Figure 1B). These findings suggest that PHV replication is inhibited within human endothelial cells.

PHV Transcription and Protein Synthesis are altered in Endothelial Cells

In order to determine why PHV replication is blocked in endothelial cells we comparatively evaluated hantavirus transcription within HUVECs. Hantavirus mRNA levels were quantitated using real-time PCR and standardized to cellular GAPDH mRNA levels (Figure 2). As previously reported, S-segment mRNA levels within NY-1V, HTNV and PHV infected endothelial cells were similar one day p.i. (28) and this similarity is reflected in comparable N-protein levels within infected cells (Figure 3). NY-1V and HTNV S-segment mRNAs increased to maximal levels 3 to 4 days p.i. while peak PHV S-segment mRNA levels were observed one day p.i. and decreased 10-20 fold 2-4 days p.i. (Figure 2).

Immunoperoxidase staining of nucleocapsid protein in infected monolayers indicated that nearly every cell contained clearly detectable levels of N protein 1 day post-infection with PHV, NY-1V and HTNV. Interestingly, we visually noted that nucleocapsid protein levels within PHV, but not HTNV or NY-1V, infected cells declined 1-4 days post infection. In order to demonstrate differences in nucleocapsid-protein levels we evaluated nucleocapsid-protein expression in NY-1V, HTNV and PHV infected endothelial cells by Western blot analysis 1-5 days p.i. Comparable levels of nucleocapsid protein were observed 1 day post-infection with NY-1V, HTNV or PHV and nucleocapsid-protein levels persisted within NY-1V and HTNV infected cells from 1-5 days post infection (Figure 3). In contrast, nucleocapsid-protein levels in PHV infected cells

decreased dramatically 2 to 4 days p.i. with no apparent nucleocapsid-protein present 5 days p.i. (Figure 3). Compared with pathogenic NY-1V and HTNV, our findings demonstrate that PHV mRNA and nucleocapsid-protein synthesis are dramatically reduced 2-5 days post-infection of human endothelial cells.

Induction of ISG56 and MxA following Hantavirus Infection

Interferon and interferon stimulated genes (ISGs) are known to regulate viral transcription and replication (37). Using real time PCR, we studied the transcription of ISG56 and MxA, which are induced by IFN secretion and binding to IFN receptors. One day post-infection we found that PHV infection of human endothelial cells directed a >225-fold increase in ISG56 mRNA compared to a 6-fold increase in ISG56 mRNA by NY-1V (Figure 4A). PHV also directed a 539-fold increase in MxA while pathogenic NY-1V or HTNV induced substantially smaller 9- or 31-fold increases in MxA, respectively, (Figure 4B). By 3 days p.i. all 3 hantaviruses induced MxA to high levels, although NY-1V directed an approximately 30-fold lower MxA response than HTNV or PHV. These studies demonstrate that non-pathogenic PHV and pathogenic NY-1V or HTNV differentially direct IFN responses 1 day post-infection of human endothelial cells. High level IFN responses induced by PHV 1 day post-infection are consistent with reduced PHV transcription, protein synthesis and replication in

human endothelial cells. These findings further suggest that NY-1V and HTNV may regulate early IFN responses during infection.

Hantaviruses Direct the Secretion of Interferon–β from Endothelial Cells

Minute amounts of secreted interferon (type-I, alpha or beta) direct the autocrine or paracrine activation of IFN receptors which amplify IFN signals and induce the high level transcription of a large number of ISGs including MxA (6, 94, 101). In order to demonstrate that hantaviruses direct MxA responses through secreted IFNs we added function blocking antibodies to IFN-α or IFN-β to the media of infected cells and assayed MxA induction 1 day post hantavirus infection. PHV directed a 10-fold higher level of MxA induction than NY-1V 1 day post-infection (Figure 5). When neutralizing antibodies to IFN-β, but not IFN-α, were added to the media, MxA induction was blocked following infection by NY-1V or PHV. This demonstrates that hantavirus infection directs the secretion of IFN-b from human endothelial cells which in turn directs MxA transcription (Figure 5).

Hantavirus Replication is IFN Sensitive

In order to determine if hantaviruses are sensitive to type-I IFN, human endothelial cells were pretreated with IFN-a (1000 IU/ml) 1 day prior to infection

with HTNV, NY-1V or PHV. IFN pretreatment completely inhibited the replication of NY-1V, HTNV and PHV while PHV replication in human endothelial cells was restricted even without added IFN (Figure 6A). These findings indicate that pathogenic hantaviruses are acutely sensitive to the prior addition of IFN and suggest that pathogenic hantaviruses need to regulate IFN responses to successfully replicate within endothelial cells.

Pathogenic Hantaviruses Develop Resistance to IFN Addition During Infection

To determine if pathogenic hantaviruses develop resistance to IFN during the course of infection, we added IFN to cells at various times following hantavirus infection (6-24 hours) and monitored viral titers 3 days post-infection. PHV replication was not detectable in endothelial cells with or without IFN treatment and the addition of IFN 6-12 hours post NY-1V or HTNV infection blocked replication almost entirely (Figure 6B). In contrast when IFN was added between 15 and 24 hours p.i. we observed a gradual increase in NY-1V and HTNV titers (Figure 6B), demonstrating the progressive insensitivity of NY-1V and HTNV replication to IFN addition. Collectively our findings are consistent with the ability of pathogenic hantaviruses to synthesize products which regulate

early IFN responses and, at later times post-infection, block the effects of IFN induced ISGs that limit viral replication.

NY-1V Co-Infection of Human Endothelial Cells Attenuates PHV-directed MxA Induction

The potential for pathogenic hantaviruses to regulate IFN responses suggested that NY-1V might suppress IFN responses directed by PHV (28). In order to test this we compared the induction of MxA during NY-1V and PHV co-infection with MxA induced by infection of each virus alone using real-time PCR. We found that PHV induced MxA over 100 fold and at least 10 fold more than NY-1V infection alone (Figure 7). In contrast, co-infecting endothelial cells with PHV and NY-1V resulted in a 66% reduction in PHV-directed MxA transcription (Figure 7). Although these findings suggest that NY-1V might repress early IFN responses directed by PHV, this experiment does not exclude the possibility that NY-1V interferes with PHV transcription.

Hantavirus Gn Protein Blocks Cellular IFN Responses

In order to determine if pathogenic hantavirus proteins are capable of regulating IFN signaling pathways, we compared the ability of the hantavirus N and Gn cytoplasmic tail proteins to regulate IFN pathway activation directed by

RIG-I and TBK1. We co-transfected cells with a constitutively active RIG-I construct containing only the amino-terminal CARD domains and a luciferase reporter driven by an interferon stimulated response element (ISRE). We evaluated the ability of NY-1V nucleocapsid or Gn cytoplasmic tail proteins to regulate RIG-I directed ISRE activation. RIG-I induced ISRE transcription approximately 130-fold over controls and expression of the NY-1V N-protein or the PHV Gn cytoplasmic tail had little effect on RIG-I directed ISRE transcription (Figure 8A). In contrast, expressing the NY-1V Gn cytoplasmic tail inhibited RIG-I directed ISRE transcription (Figure 8A) and co-transfecting increasing amounts of the NY-1V Gn-tail expression plasmid resulted in a concomitant decrease in RIG-I directed ISRE transcription (>90 %) (Figure 8B). These results indicate that the NY-1V Gn cytoplasmic tail blocks RIG-I directed transcriptional responses from ISRE containing promoters.

Sequence Differences within the Gn-tails of NY-1V and PHV

An analysis of NY-1V and PHV Gn cytoplasmic tails revealed the presence of 41 different residues in their 142 amino acid cytoplasmic tails (27% divergence; Figure 8C). There are notable changes within the Gn-tails which include charge changes, proline insertions, tyrosine differences and the presence of an additional cysteine at residue 128 within the PHV Gn-tail. However, the broad divergence of PHV and NY-1V Gn-tails does not delineate a specific

residue change or domain that might account for the differential regulation of RIG-I directed responses.

NY-1V Gn-tail Regulates TBK1 Directed Transcription from ISRE and IFN-β Promoters

TBK1 is a downstream effector of RIG-I activation and TBK1 activation is required for ISRE and IFN-b transcriptional responses. To determine whether the Gn cytoplasmic tail inhibits IFN signaling upstream or downstream of TBK1, we determined whether hantavirus proteins regulate TBK1 directed transcriptional responses. We determined the effect of the NY-1V Gn cytoplasmic tail on transcriptional responses directed by the complete IFN-b promoter. TBK1 directed transcription from the IFN-b promoter >40-fold while co-expression of the NY-1V Gn cytoplasmic tail inhibited TBK1 directed IFN-b transcriptional responses >95% (Figure 9A). Transfecting identical amounts of NY-1V N or PHV Gn cytoplasmic tail expression plasmids had little effect on TBK1 directed IFN-b transcription (Figure 9A). Transfecting cells with increasing amounts of NY-1V Gn cytoplasmic tail resulted in a dose-dependent decrease in TBK1 directed transcription from the IFN-β promoter (Figure 9B).

We similarly found that TBK1 activated ISRE transcription approximately 190-fold over controls and that co-expression of the NY-1V Gn cytoplasmic tail resulted in a >90% reduction in TBK1 directed ISRE transcription (Figure 10). In

contrast, co-expression of either the NY-1V N-protein or the PHV Gn cytoplasmic tail had little or no effect on TBK1 directed ISRE transcriptional responses (Figure 10). Similar to RIG-I, co-transfecting cells with an increasing amount of NY-1V Gn cytoplasmic tail resulted in a dose dependent inhibition of TBK1 directed transcription (Figure 10). These findings indicate that expression of the NY-1V Gn cytoplasmic tail blocks transcription from ISRE and promoters at or downstream of TBK1 complex.

NY-1V Gn-tail Regulates Transcription Upstream of IRF-3 Phosphorylation

Activated TBK1 phosphorylates IRF-3 and phosphorylated IRF-3 dimerizes and translocates to the nucleus where it directs transcriptional responses (39). To determine if the NY-1V Gn-tail regulates IFN responses upstream of downstream of IRF-3 phosphorylation we induced ISRE transcription using a constitutively active phospho-mimetic form of IRF-3 (IRF-3 5D) (65). IRF-3 5D expression resulted in a >70-fold induction of the ISRE reporter and co-expression of either NY-1V or PHV G1-tails failed to inhibit IRF-3 5D directed transcriptional responses (Figure 11). These findings indicate that the NY-1V Gn-tail is incapable of inhibiting phospho-IRF-3 directed transcriptional responses and suggest that Gn regulates IFN transcriptional responses upstream of IRF-3 phosphorylation at the level of the TBK1 complex.

The NY-1V Gn Cytoplasmic tail Inhibits IFN-β and NF-κB transcriptional responses

We have shown that the NY-1V Gn cytoplasmic tail inhibits RIG-I and TBK1 directed IFN-β transcriptional responses while the Gn-tail from the non-pathogenic hantavirus PHV failed to regulate transcription (3). IFN-β induction requires IRF-3 phosphorylation as well as NF-κB activation and here we tested whether expression of the NY-1V Gn-tail specifically inhibited NF-κB directed transcriptional responses. Cells transfected with a plasmid expressing the NY-1 virus Gn cytoplasmic tail inhibited transcription from both IFN-β and NF-κB luciferase reporters (Figure 12 A, B). In contrast, cells transfected with increasing amounts of the PHV Gn cytoplasmic tail failed to regulate IFN-β or NF-κB transcriptional responses and instead the PHV Gn-tail slightly enhanced transcriptional responses (Figure 12 A, B).

TRAF2 reportedly forms a complex with TBK1 and activates NF-κB (90). In order to determine whether the NY-1V Gn-tail blocks TRAF2 directed responses we co-transfected cells with the NY-1V or PHV Gn-tail and TRAF2 expression plasmids and assessed NF-κB transcriptional responses using a luciferase reporter (Figure 12 C). TRAF2 over-expression activated κB luciferase reporter gene expression over 50-fold and co-expression of the PHV Gn-tail had no effect on NF-κB activation. In contrast, co-expression of the NY-1V Gn-tail resulted in the dose dependent inhibition of TRAF2 directed NF-κB activation

(Figure 1 2C). These results indicate a functional difference in the ability of the pathogenic NY-1V Gn-tail and non-pathogenic PHV Gn-tail to regulate TBK1 and TRAF2 directed NF-κB activation.

The NY-1V Gn Cytoplasmic tail Binds TRAF3

The NY-1V Gn-tail blocks IFN directed transcriptional responses upstream of IRF-3 at the level of the TBK1 complex. To determine if the NY-1V Gn-tail directly binds TBK1 or TRAF3 proteins we co-expressed the NY-1V or PHV Gn-tail in the presence of co-expressed TBK1 or TRAF3 and assayed for protein co-immunoprecipitation. Although TBK1 and the Gn-tails of NY-1V and PHV were detected from cell lysates, neither the NY-1V nor PHV Gn-tail was able to Co-precipitate TBK1 (Figure 13 A). In contrast, the NY-1V, but not PHV, Gn-tail co-precipitated TRAF3 as determined by TRAF3 Western blotting (Figure 13 B). The NY-1V Gn-tail is proteasomally degraded, and Figure 13 C demonstrates that Gn-tail co-precipitation of TRAF3 was dependent on the presence of the proteasome inhibitor MG132. This further demonstrates that co-precipitation of TRAF3 was specific and dependent on the presence of the NY-1V Gn-tail. These findings indicate that the NY-1V Gn-tail binds TRAF3 and that TRAF3 binding differentiates the pathogenic NY-1V Gn-tail from the Gn-tail of the non-pathogenic hantavirus PHV.

The NY-1V Gn-tail Binds the N-terminal Domain of TRAF3 and TRAF2

TRAF3 contains a unique C-terminal domain that mediates TRAF3 binding to IPS-1 and links upstream signals to downstream TBK1 directed IFN induction (99). To determine if the NY-1V Gn-tail interacts with N- or C-terminal TRAF domains we evaluated the ability of the NY-1V Gn-tail to bind a C-terminally truncated TRAF3 protein (TRAF3-N415). In contrast to the PHV Gn-tail, we found that the NY-1V Gn-tail co-precipitated the truncated TRAF3 protein (Figure 14 A). These findings indicate that the N-terminal domain of TRAF3 was sufficient for binding to the NY-1V Gn-tail, and further suggests that the NY-1V Gn-tail might bind to conserved N-terminal domains of additional TRAFs (34).

The N-terminal domain of TRAF3 can be functionally replaced by the corresponding N-terminus of other TRAFs (34, 99). Since our data indicates that the NY-1V Gn-tail regulates TRAF2 transcriptional responses we evaluated whether the Gn-tail binds the N-terminal domain of TRAF2 (TRAF2-N355). Figure 3B demonstrates that the TRAF2 N-terminus was co-precipitated by the NY-1V Gn-tail but not the PHV Gn-tail (Fig 14 B). These results suggest that the NY-1V Gn cytoplasmic tail binds to the N-terminal domains of both TRAF2 and TRAF3. The interaction of the NY-1V Gn-tail with TRAF2 and TRAF3 provides a redundant mechanism for the regulation of IFN-β transcriptional responses by pathogenic hantaviruses.

TBK1 Co-precipitation of TRAF3 is inhibited by the NY-1V Gn cytoplasmic tail

TBK1 binding to TRAF3 results in the formation of a signaling complex that directs downstream IFN-β transcriptional responses (32, 77). The NY-1V Gn-tail also binds TRAF3 suggesting that the NY-1V Gn-tail might disrupt TRAF3 binding to TBK1. Figure 15 indicates that co-expression of the NY-1V Gn-tail along with TRAF3 and TBK1 completely abolished TBK1 co-precipitation of TRAF3 compared to a GAL4 control. This result suggests that the NY-1V Gn-tail prevents TBK1 interactions with TRAF3 and is consistent with the ability of the NY-1V Gn-tail to inhibit TBK1 directed IFN-β transcriptional responses. These findings suggest a mechanism by which the NY-1V Gn-tail regulates cellular IFN pathway activation at early times after infection.

Infection with NY-1 virus disrupts TBK1-TRAF3 complex formation

PHV strongly induces the transcription of ISGs one day post-infection while NY-1V, regulates early IFN responses (3, 28, 59). Since expression of the NY-1V Gn-tail disrupted TBK1-TRAF3 interactions, we assessed whether infection by NY-1V similarly disrupted TBK1-TRAF3 interactions. TBK1 co-precipitated TRAF3 in PHV infected cells however TBK1 failed to co-precipitate TRAF3 in NY-1V infected cells (Figure 16). These findings indicate that similar to expressing the NY-1V Gn-tail, infection by NY-1V inhibits TBK1-TRAF3 interactions. These findings suggest pathogenic hantavirus regulation of host-cell

IFN-β induction and ISG expression is a consequence of Gn-tail interactions with TRAF3 that block TRAF3-TBK1 complex formation.

FIGURES AND LEGENDS

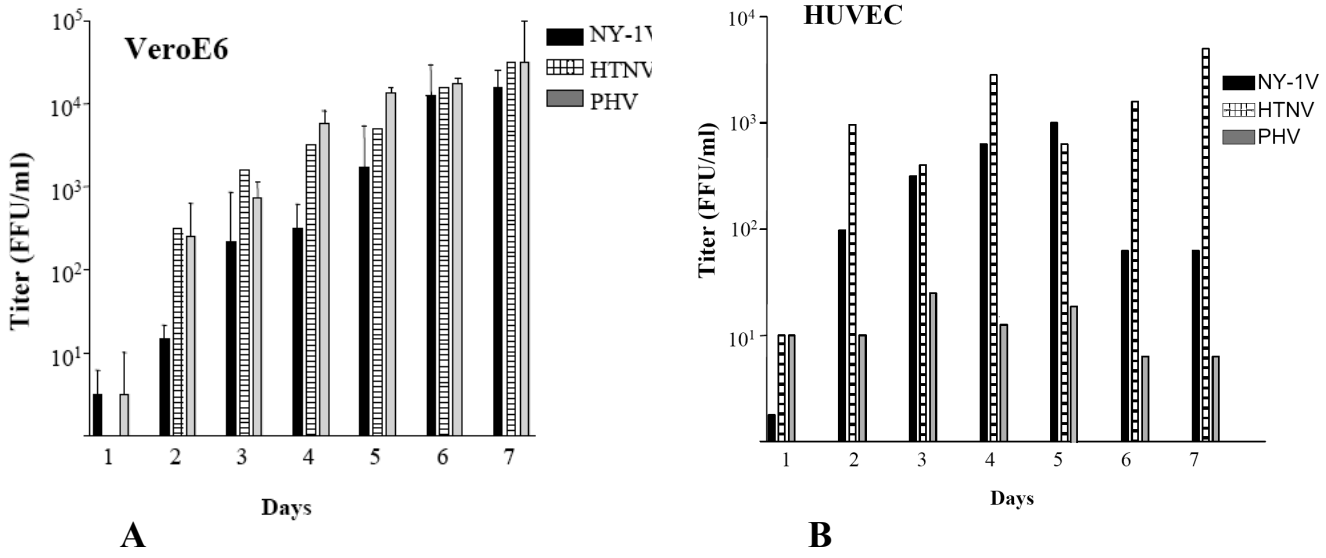

Figure 1. Hantavirus Replication in HUVECs and Vero E6 Cells.

Vero E6 cells (A) and HUVECs (B) were infected with NY-1V, HTNV or PHV at a multiplicity of infection (MOI) of 1. Viral titers in the supernatant of infected cells were analyzed 1 to 7 days post-infection by infectious focus assay (25). Days post-infection are indicated on the x-axis and titers are represented as FFU/ml.

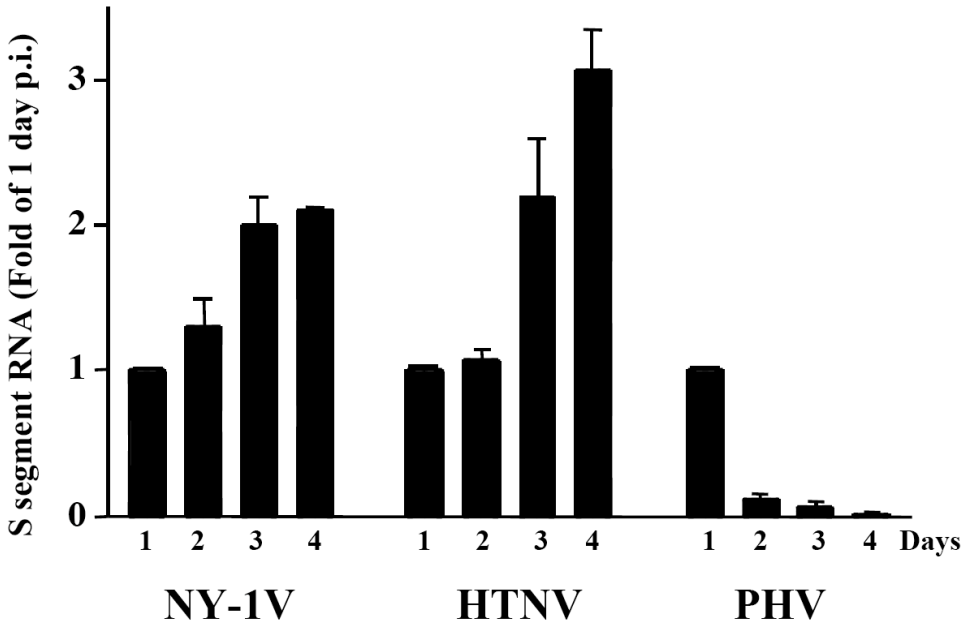

Figure 2. Kinetics of S Segment RNA synthesis during hantavirus infection.

HUVECs were mock infected or infected with NY-1V, HTNV, or PHV (MOI of 1). S segment RNA levels were determined by quantitative real-time PCR using hantavirus S-segment specific primers 1-4 days post-infection and responses from duplicates were normalized to GAPDH mRNA levels. Experiments were performed twice with similar results and mRNA levels are expressed as the fold change from 1 day levels.

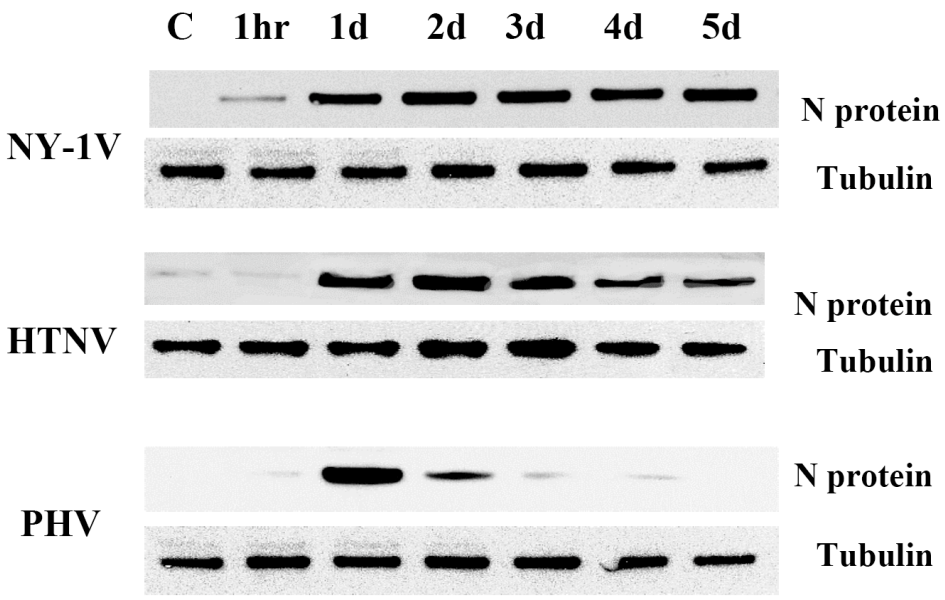

Figure 3. Western blot analysis of N-protein Expression.

HUVECs were infected with NY-1V, HTNV or PHV (MOI of 1) or mock infected (C). Cells were lysed one hour or 1-5 days post-infection as indicated. Total protein levels were determined and an equivalent amount of whole cell lysate was separated by 10% SDS-PAGE. Proteins were detected by Western blotting using anti-nucleocapsid polyclonal rabbit antibody or anti-tubulin monoclonal antibody (Sigma), species-specific secondary antibodies (HRP-conjugated) and detected using ECL (Amersham).

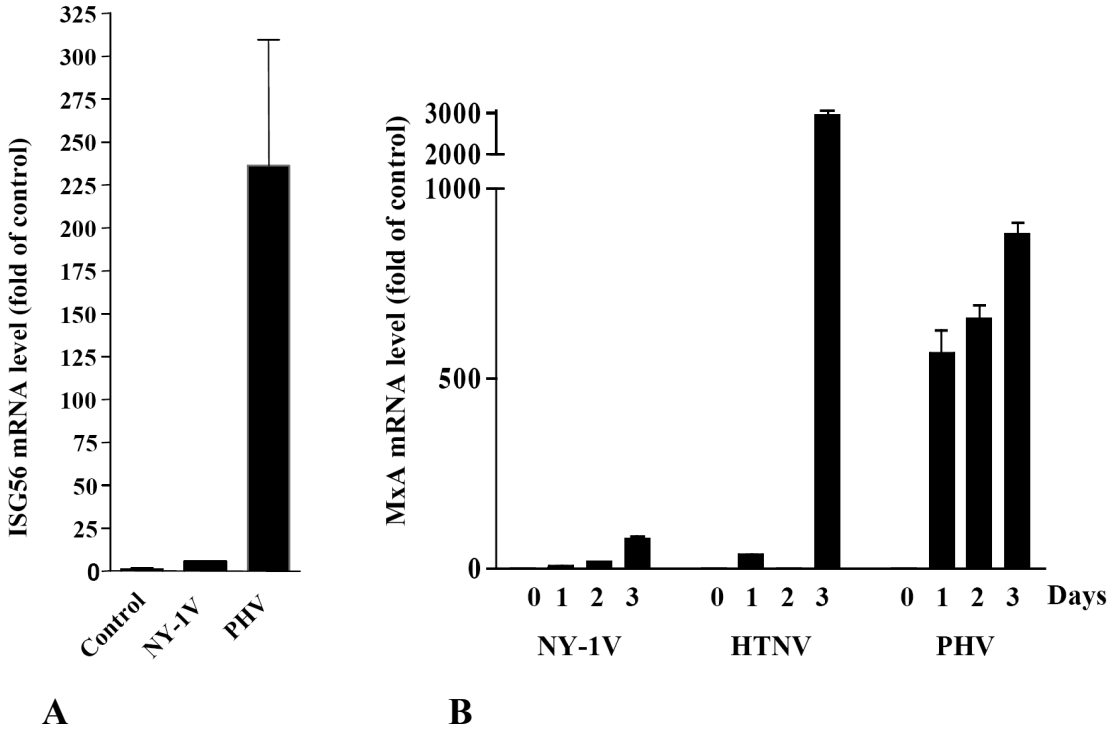

Figure 4. Kinetics of MxA and ISG56 mRNA induction during hantavirus infection.

HUVECs were infected with NY-1V, PHV (MOI of 1) or mock infected. One day post-infection ISG56 (A) or MxA (B) mRNA levels were determined, relative to mock infected controls, using quantitative real-time PCR and normalized to GAPDH mRNA levels. MxA mRNA levels were quantified 0, 1, 2 and 3 days post-infection.

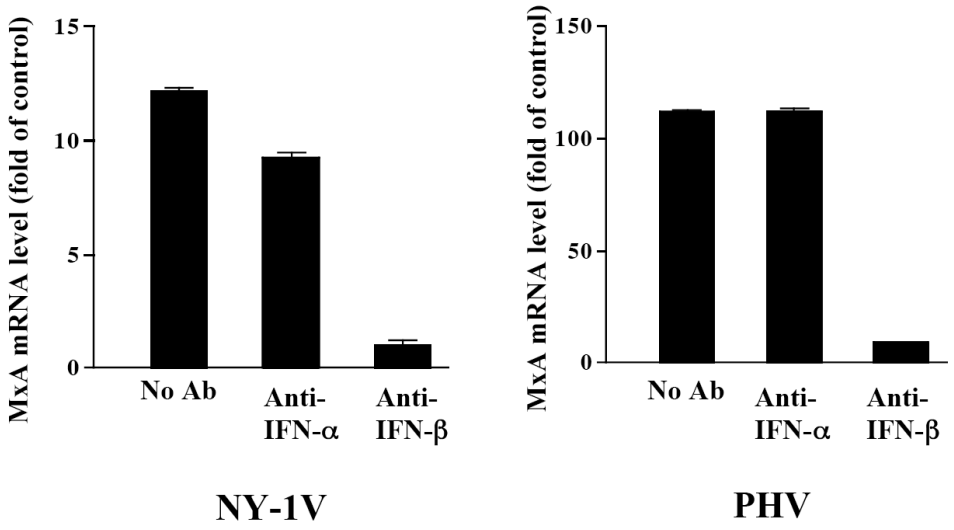

Figure 5. Antibody to IFN-β Inhibits the Hantavirus Directed MxA Induction.

HUVECs were infected at an MOI of 1 with NY-1V or PHV or mock infected. Following adsorption, anti-IFN-α or anti-IFN-β neutralizing antibodies were added to the media as indicated and MxA mRNA levels were quantified by real-time PCR as described above. MxA levels are shown as the fold increase over mock infected controls. The scale of the Y axes for Y-1V and PHV differ by 10 fold (3).

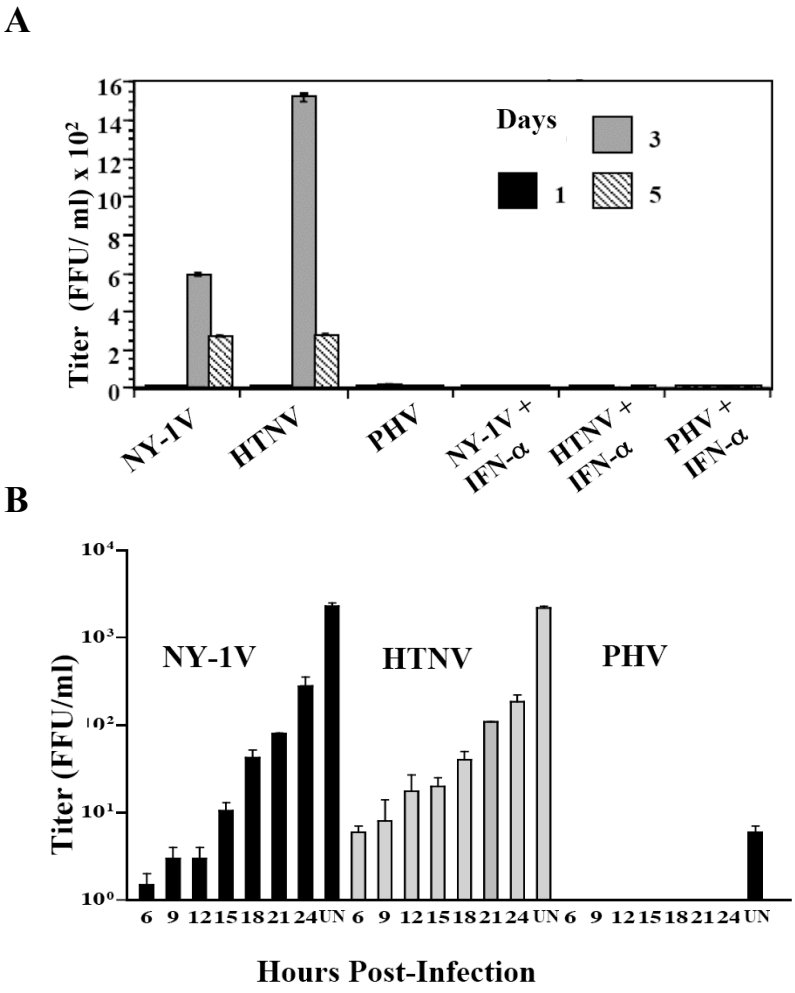

Figure 6. Hantavirus Replication in the Presence of type-I Interferon.

(A) Vero E6 cells were pretreated in duplicate with 1000 IU/ml IFN-α or left untreated for 24 hours prior to infection with NY-1, HTN, and PH viruses (MOI of 1) or mock infection. Hantavirus titers were determined using a focus assay 0, 1, 3, and 5 days post-infection as previously described (25). (B) HUVECs were infected as in 6A prior to the addition of 1000 IU/ml of IFN-α 6-24 h post-infection or were untreated (UN) as indicated. Three days post-infection, cell supernatants were titered on Vero E6 cells using a focus assay (16).

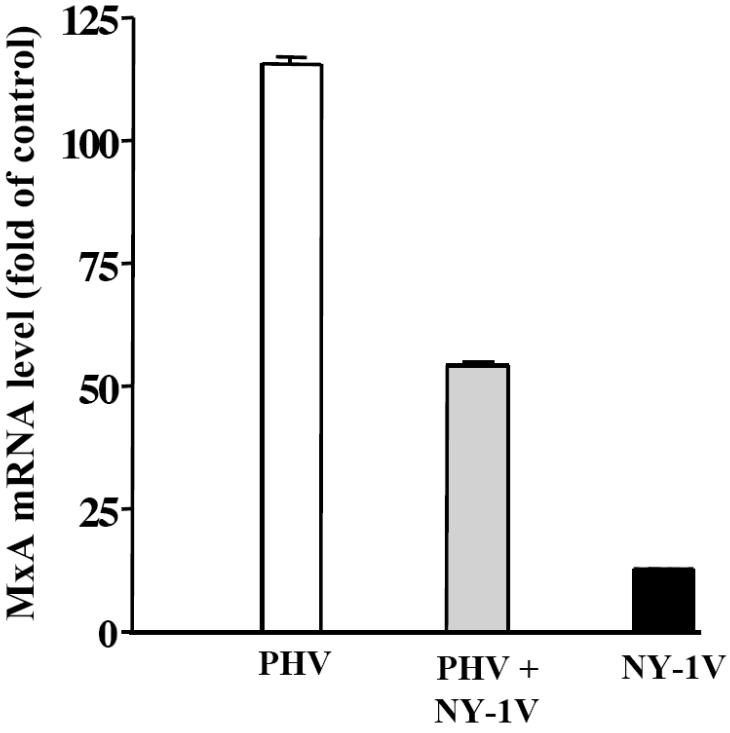

Figure 7. NY-1V Co-Infection Attenuates PHV directed MxA induction.

HUVECs were mock infected, infected with NY-1V, PHV (MOI of 0.5), or co-infected with NY-1V and PHV (MOI of 0.5 each), in duplicate. One day post-infection, MxA mRNA levels were quantified by real-time PCR, standardized to GAPDH mRNA levels as described above and are reported as the fold increase in mRNA levels over mock infected controls.

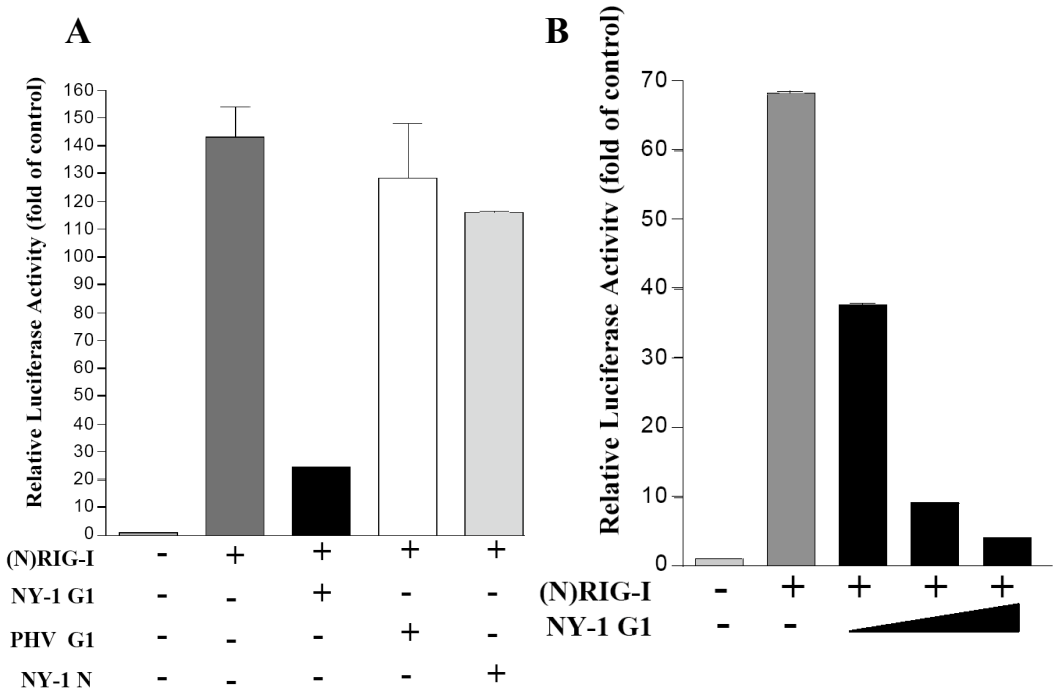

Figure 8. NY-1V Gn cytoplasmic tail inhibits RIG-I directed ISRE activation.

(A) HEK 293 cells were transfected with an ISRE driven luciferase reporter construct with or without co-transfection of the (N)RIG-I expression plasmid (500 ng). Cells were co-transfected with plasmids expressing the NY-1V or PHV Gn cytoplasmic tail, or the NY-1V N-protein (2 μg). (B) Cells were co-transfected with the (N)RIG-I expression vector (250 ng) and increasing amounts of plasmid expressing the NY-1V Gn cytoplasmic tail (0.5, 1 or 2 μg) or control empty vector in order to transfect cells with constant amounts of total DNA. Two days post-transfection, cells were lysed, luciferase activity was assayed and the fold increase in luciferase activity over controls which were not transfected with (N)RIG-I was reported after normalizing to *Renilla* luciferase levels.

Figure 8C

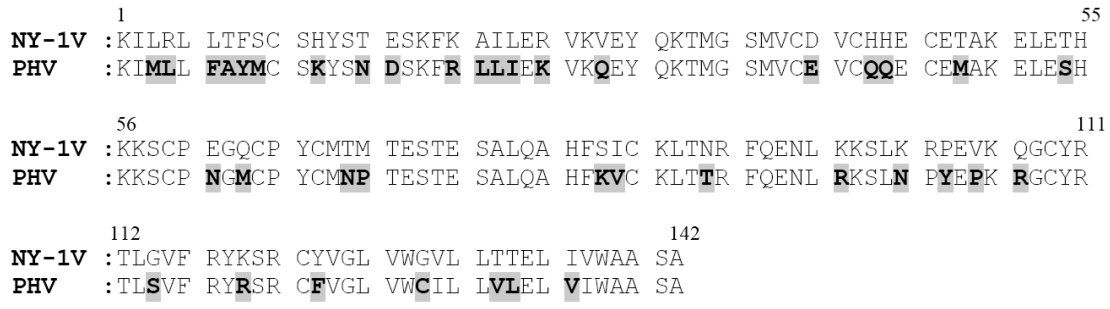

Figure 8. NY-1V Gn cytoplasmic tail inhibits RIG-I directed ISRE activation.

(C) Amino acid alignment of 142 residue Gn-tail sequences from NY-1V (Gn 510-652) and PHV (Gn 513-655). PHV residues which differ from NY-1V are highlighted and bolded.

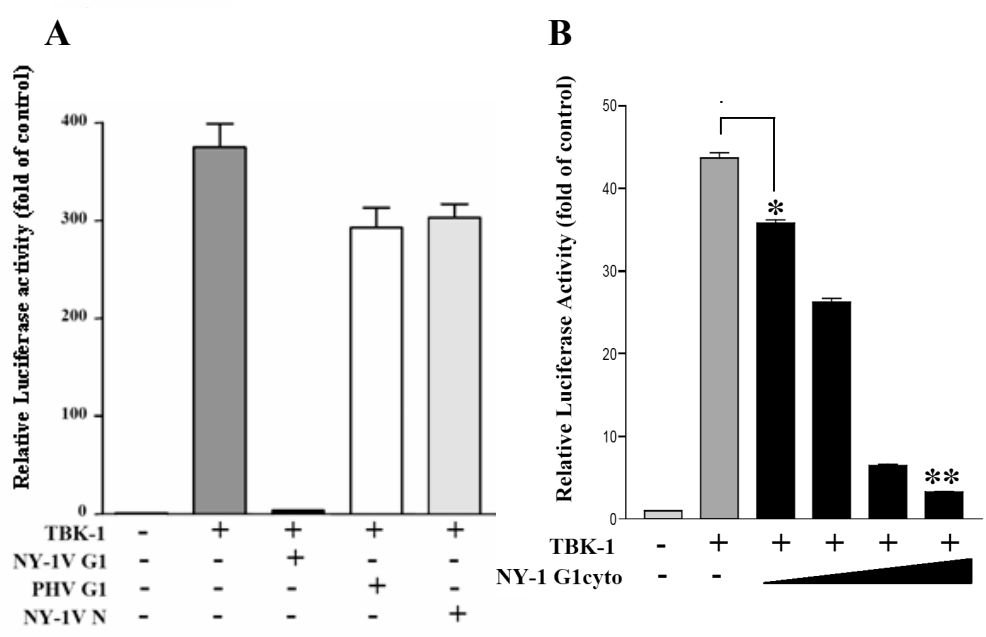

Figure 9. Hantavirus Gn cytoplasmic tail disrupts IFN-β promoter activation.

(A) Duplicate wells of HEK 293 cells were transfected with an IFN-β promoter driven luciferase reporter with or without a TBK1 expression vector (500 ng). Cells were co-transfected with equal amounts of NY-1V or PHV Gn cytoplasmic tail or NY-1V N-protein expression vectors (4 μg) as indicated. Luciferase activity was determined 48 h post-transfection and normalized to *Renilla* luciferase activity. Luciferase activity is reported as the fold increase over controls not transfected with TBK1. (B) Cells were transfected with the TBK1 expression vector as above (250 ng) along with an increasing amount of plasmid expressing the NY-1V Gn cytoplasmic tail (0.5, 1, 2 or 4 μg) or control empty vector in order to transfect cells with a constant amount of DNA. Differences were statistically significant (* = $P < 0.05$, ** = $P < 0.001$).

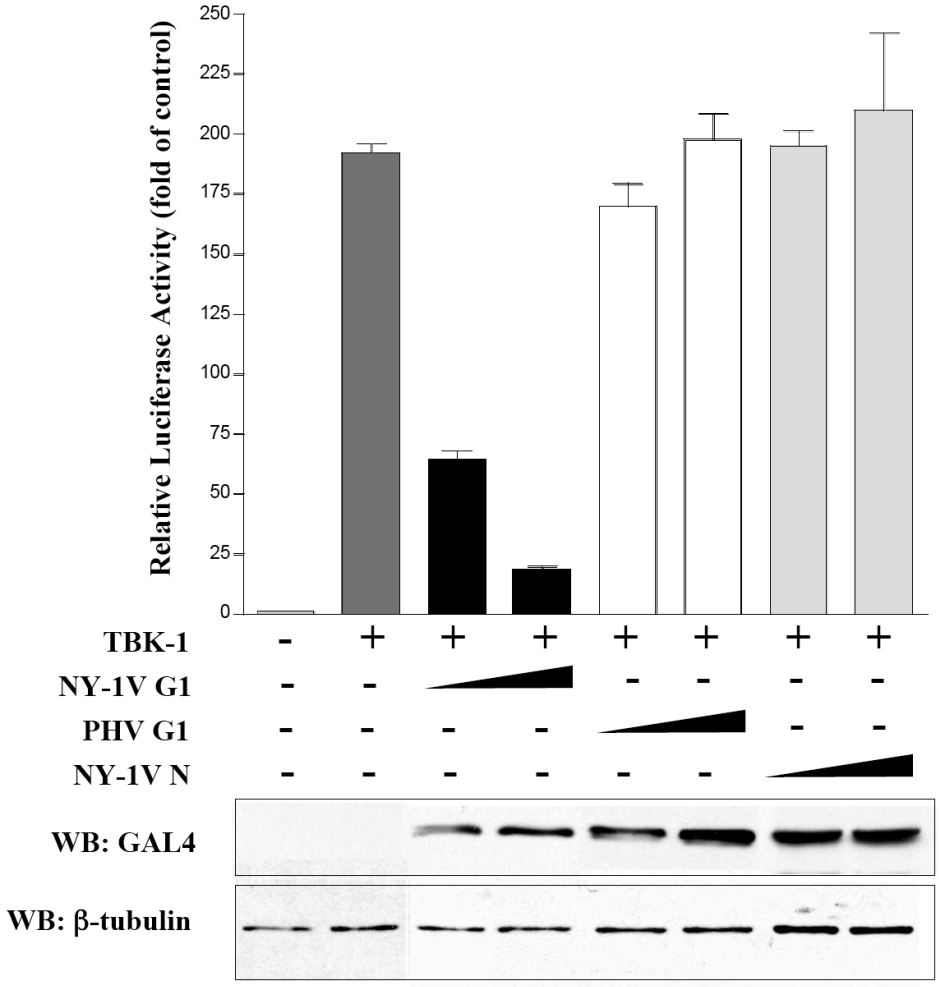

Figure 10. NY-1V Gn cytoplasmic tail blocks TBK1 directed ISRE activation.

ISRE luciferase reporters were transfected into HEK 293 cells with or without TBK1 expression plasmids (500 ng). Cells were co-transfected with an increasing amount of NY-1V Gn cytoplasmic tail, PHV Gn cytoplasmic, or NY-1V N-protein expression vectors (1 or 2 μg) or empty vector in order to transfect cells with a constant amount of DNA. Luciferase reporter activity was assayed 48 h post-transfection, normalized to *Renilla* luciferase activity, and is reported as the fold increase over controls lacking TBK1 activation. Protein expression levels, cells were similarly evaluated by Western blot 48 hours p.i. from parallel, comparably transfected monolayers using an anti-Gal4 antibody and β-tubulin levels were analyzed by Western blot as internal controls.

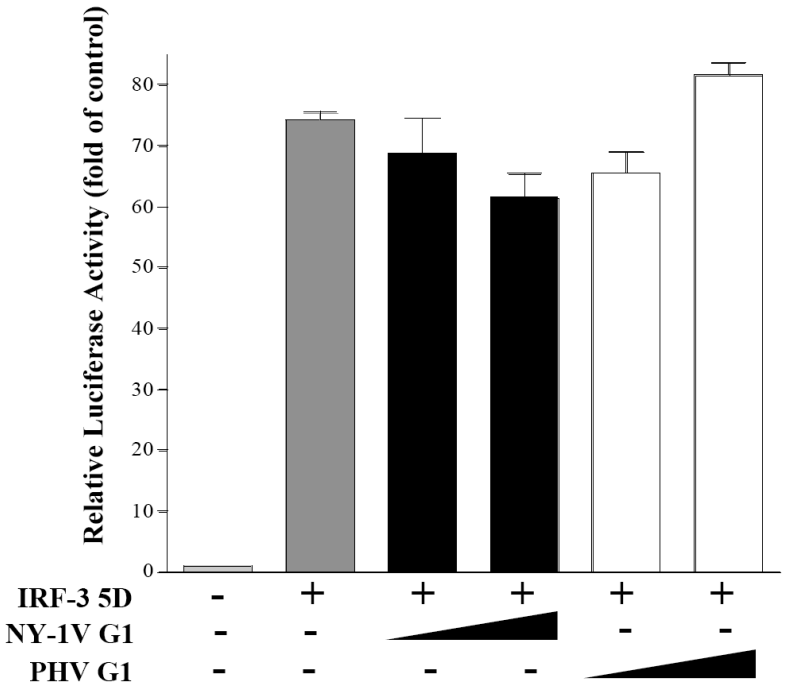

Figure 11. NY-1V Gn Tail Inhibits Transcription Upstream of IRF-3 Phosphorylation.

ISRE luciferase reporters were transfected into HEK 293 cells with or without IRF-3 5D expression plasmids (500 ng). Cells were co-transfected with the NY-1V or PHV Gn cytoplasmic tail, or NY-1V N-protein expression vectors as indicated (2 μg). Luciferase reporter activity was assayed as in Figure 8, 48 h post-transfection, and is reported as the fold increase over controls lacking IRF-3 5D.

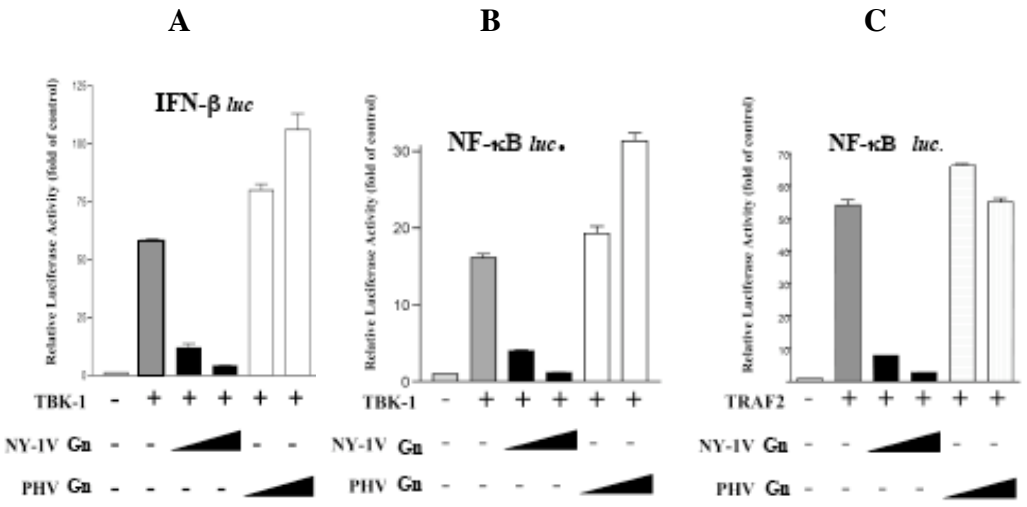

Figure 12 NY-1V Gn cytoplasmic tail Inhibits TBK1 and TRAF2 Directed NF-κB Activation

HEK 293 cells were transfected with IFN-β promoter (A) or NF-κB (B, C) luciferase reporters with or without TBK1 or TRAF2 expression vectors. Where indicated, cells were transfected with increasing amounts of NY-1V or PHV Gn cytoplasmic tail expression vectors or empty vector in order to transfect cells with a constant amount of DNA. Luciferase reporter activity was assayed 48 hours post-transfection, normalized to *Renilla* luciferase levels, and is reported as fold-increase relative to controls lacking TBK1 or TRAF2 activation.

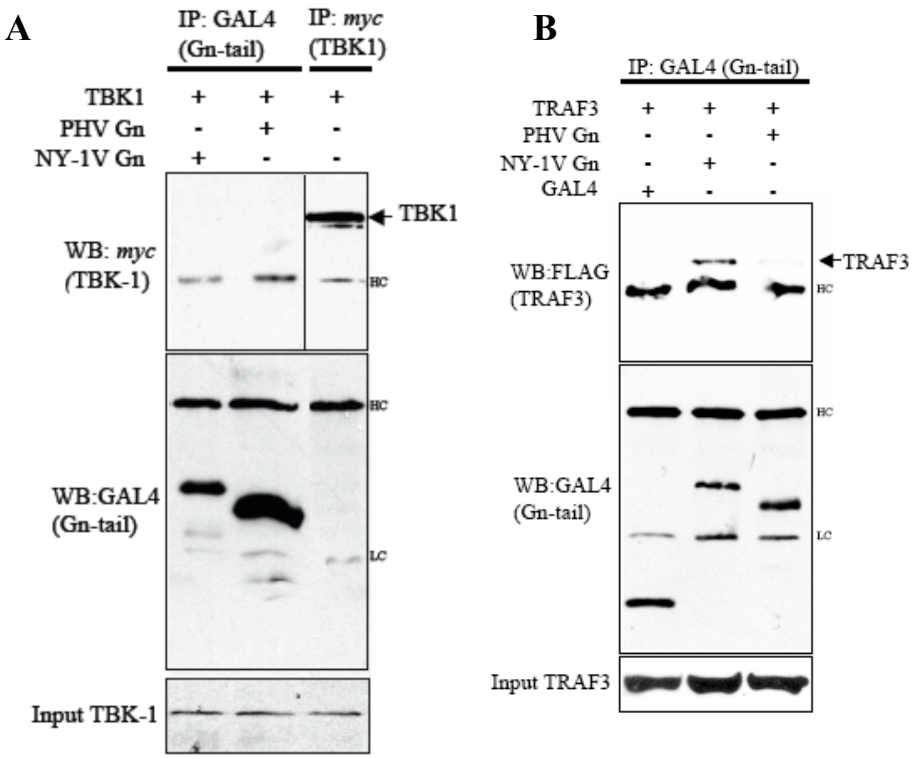

Figure 13. The NY-1V Gn-tail binds TRAF3

(A) HEK 293 cells were transfected with TBK1, NY-1V Gn-tail or PHV Gn-tail expression plasmids as indicated. Two days post-transfection GAL4- or *myc*-tagged proteins were immunoprecipitated (IP) with anti-GAL4 or anti-*myc* antibodies. Immunocomplexes were isolated on protein A/G agarose beads and immunoprecipitated proteins were detected by anti-GAL4 (Gn-tail) or anti-*myc* (TBK1) Western blotting (WB). (B) HEK 293 cells were transfected with TRAF3, NY-1V Gn-tail, PHV Gn-tail or GAL4 expression plasmids as indicated. FLAG-tagged TRAF3 protein expression was analyzed by anti-FLAG Western blotting and is shown in the bottom panel. GAL4 tagged Gn-tail proteins were immunoprecipitated and immunocomplexes were isolated as in 1A. Immunoprecipitated Gn-tail proteins were analyzed by anti-GAL4 Western blotting (center panel) and co-immunoprecipitated FLAG-TRAF3 protein was analyzed by anti-FLAG western blotting (top panel).

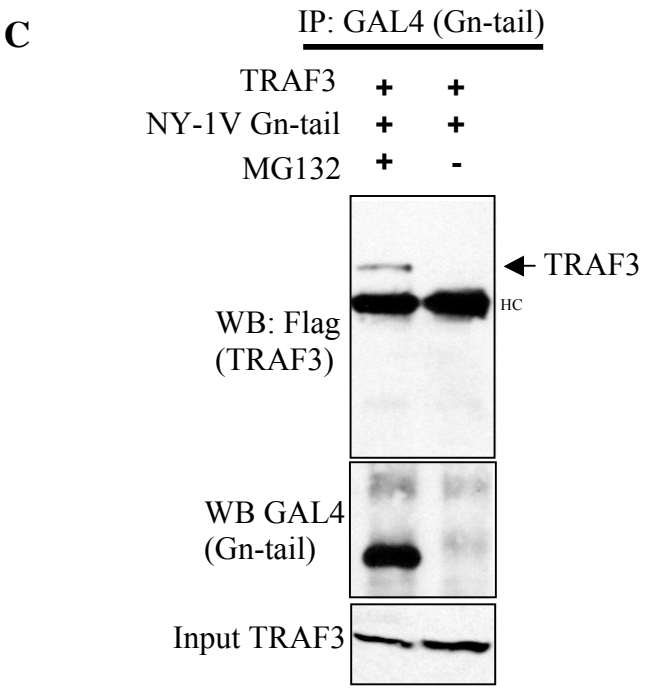

Figure 13. The NY-1V Gn-tail binds TRAF3

(C) The co-precipitation of TRAF3 by the NY-1V Gn-tail was performed in the presence or absence of MG132. IgG heavy chain (HC), light chain (LC).

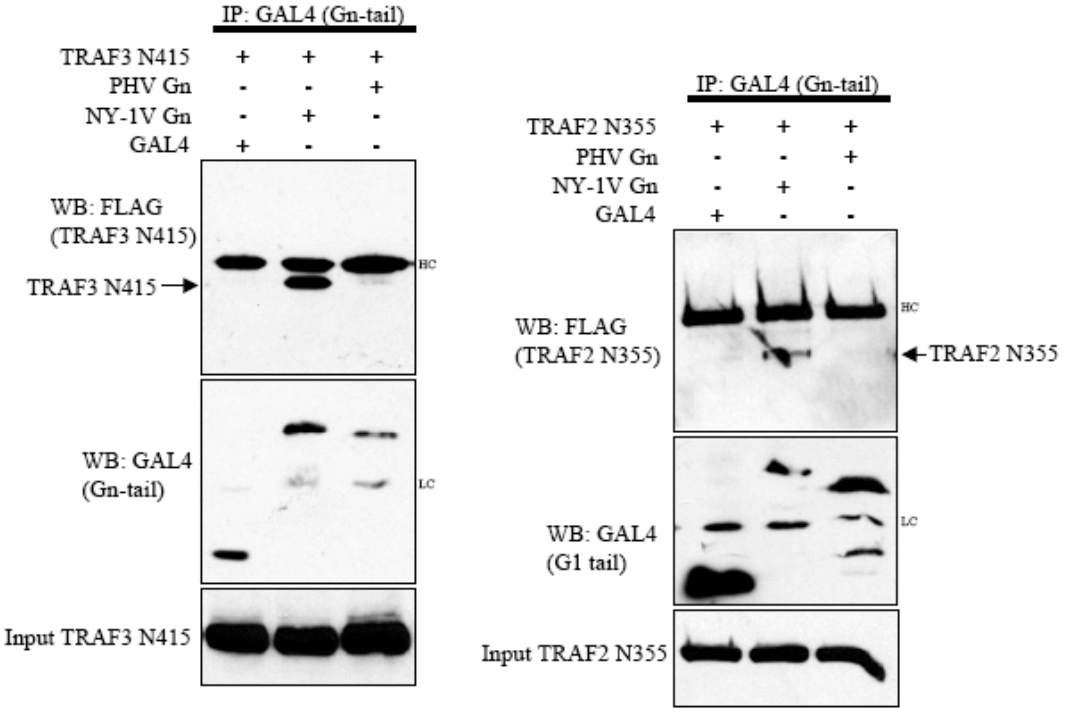

Figure 14 The NY-1V Gn cytoplasmic tail Binds the N-terminal Domain of TRAF2 and TRAF3

HEK 293 cells were co-transfected with GAL4, NY-1V-Gn or PHV-Gn expression plasmids along with FLAG-TRAF3 (N415) (A) or FLAG-TRAF2 (N355) (B). Two days post-transfection, and following anti-GAL4 antibody immunoprecipitation (IP) NY-1V and PHV Gn-tail expression was analyzed by anti-GAL4 Western blotting (center panels). Immunocomplexes were isolated on protein A/G agarose beads, and co-immunoprecipitated TRAF3 (N415) or TRAF2 (N355) proteins were analyzed by anti-FLAG Western blotting (WB) (top panels). TRAF3 (N415) or TRAF2 (N355) expression was determined by anti-FLAG Western blotting (lower panels). IgG heavy chain (HC) and light chain (LC) are indicated.

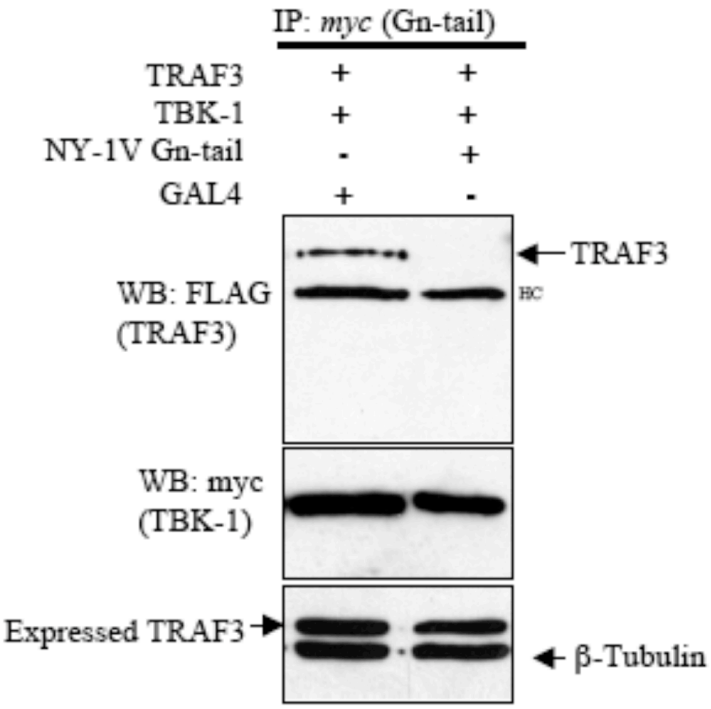

Figure 15 Expression of the NY-1V Gn cytoplasmic tail disrupts TBK1-TRAF3 interactions

HEK 293 Cells were co-transfected with TBK1 and TRAF3 expression vectors, and either NY-1V Gn-tail or GAL4 expression vectors. Two days post-transfection, cells were lysed and TBK1 was immunoprecipitated (IP) using a monoclonal anti-*myc* antibody. Co-precipitated FLAG-TRAF3 was detected by anti-FLAG Western blotting (WB) (top panel). TBK1 and TRAF3 expression was determined by anti-*myc* or anti-FLAG Western blot (lower panels).

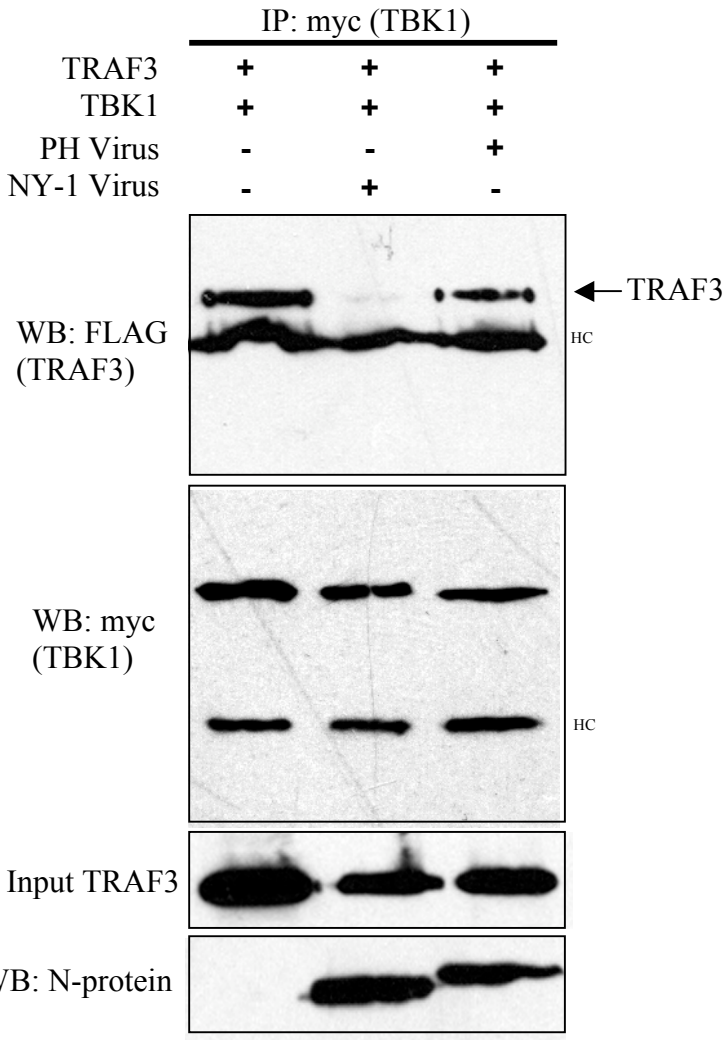

Figure 16 NY-1V but not PHV infection disrupts TBK1-TRAF3 interactions

Vero E6 cells were transfected with TBK1 and TRAF3 expression plasmids and 24 hours post-transfection cells were infected with NY-1V, PHV or mock infected. One day post-infection cells were lysed and TBK1 was immunoprecipitated (IP) with anti-*myc* antibody. Co-precipitated TRAF3 was detected by anti-FLAG Western blotting (WB). Immunoprecipitated TBK1 and input TRAF3 were determined by Western blot (center panels). NY-1V and PHV infected cells were determined by Western blotting for nucleocapsid protein (N-protein) 24 hours post-infection using an anti-N-protein rabbit polyclonal antiserum (bottom panel).

CHAPTER 4:

DISCUSSION

Section 1: The Pathogenic Hantaviruses Gn Cytoplasmic tail is a Type-I Interferon Antagonist

Hantaviruses predominantly infect endothelial cells and cause two diseases with defects in vascular endothelial barrier functions (14, 44). There are a few hantaviruses which are not associated with any human disease although there is little information about the replication of non-pathogenic hantaviruses in human endothelial cells (120, 129). The cellular entry of pathogenic and non-pathogenic hantaviruses reportedly requires different integrin receptors with differing roles in vascular permeability, however non-pathogenic hantaviruses still enter human endothelial cells (24, 130). This suggests that at one level intracellular processes are likely to determine the pathogenic potential of specific hantaviruses. In contrast to pathogenic hantaviruses, the non-pathogenic hantavirus PHV induces early IFN responses and PHV replication is inhibited in human endothelial cells. Findings presented here indicate that expression of the Gn cytoplasmic tail from pathogenic NY-1V, but not PHV, regulates the induction of cellular IFN responses. These findings further suggest that the NY-1V Gn-tail disrupts TBK1-TRAF3 complex formation by binding to TRAF3 and that Gn-tail is a primary determinant of hantavirus pathogenesis.

DNA array data suggested that PHV infection of human endothelial cells is unique from that of HTNV and NY-1V (28). PHV directs strong IFN responses within endothelial cells 1 day post-infection which are absent following infection

by HTNV or NY-1V (28). This prompted us to compare pathogenic and non-pathogenic hantavirus RNA synthesis and replication within human endothelial cells. Our findings demonstrate that PHV RNA and protein synthesis are primarily restricted to the first day of hantavirus infection and decrease dramatically 2-5 days post-infection of human endothelial cells. Our results also demonstrate that PHV replication is nearly completely blocked following infection of human endothelial cells. This contrasts with pathogenic HTNV and NY-1V which continue to synthesize viral mRNA and protein 1-5 days post-infection and successfully replicate within human endothelial cells. Consistent with a role for IFN in regulating PHV replication within human endothelial cells, PHV replicates successfully in Vero E6 cells which lack a type-I IFN genetic locus (15, 123). The successful replication of pathogenic hantaviruses in endothelial cells, the absence of early ISG induction by HTNV or NY-1V and the inhibition of PHV directed ISG responses by NY-1V co-infection suggest that pathogenic hantaviruses regulate early IFN responses following infection. Findings presented here suggest that early PHV-directed interferon responses restrict PHV's ability to replicate within endothelial cells and provide a strong rationale for why PHV is not a human pathogen.

The ability of type-I interferon to protect endothelial cells from HTNV infection has been reported (82). Pretreating endothelial cells with type-I interferon also inhibits NY-1V and PHV replication demonstrating that

pathogenic and non-pathogenic hantaviruses are sensitive to the effects of interferon added prior to infection. In fact, addition of IFN up to 12 h post-infection still blocked NY-1V and HTNV replication and suggested a rationale for why hantaviruses need to regulate the early induction of IFN responses by endothelial cells in order to replicate. Interestingly, addition of IFN 15-24 hours post-infection coincided with an increase in NY-1V and HTNV replication suggesting that viral products synthesized 12-24 hours post-infection, compensate for IFN induced responses. These findings suggest that pathogenic hantaviruses have at least two means for regulating innate cellular responses, one which inhibits the early induction of IFN and a second which permits hantavirus replication in the presence of added IFN or high levels of ISGs at later times post-infection. Currently there is no information on hantavirus proteins that might temper the effects of IFN on hantavirus replication or regulate the function of ISGs.

MxA is an ISG that reportedly blocks PUUV, TULV, and HTNV replication when constitutively expressed in cells prior to infection (20, 33, 49) and we have demonstrated an inverse correlation between the induction of MxA and PHV replication. The early high level MxA responses directed by PHV, but not NY-1V or HTNV, suggest that MxA alone could be responsible for limiting PHV transcription and replication within endothelial cells. High levels of MxA are also induced by pathogenic hantaviruses 2-4 days post-infection of human

endothelial cells but MxA induction at this point appears to have little effect on NY-1V or HTNV replication. These findings are consistent with clinical data indicating that only early IFN treatment is effective against hantavirus disease (4). Collectively this data suggests that hantaviruses are unable to compensate for preinduced ISGs or even preexisting MxA protein but that during the course of infection, hantaviruses produce compensatory products which counter the effects of MxA and presumably other ISGs that might otherwise limit hantavirus replication. (28, 49, 59). These findings indicate that hantavirus regulation of IFN responses is a transient early inhibitory effect and that pathogenic hantaviruses have the ability to replicate in the presence of IFN induced ISG responses at later times post-infection (28, 59). The means by which pathogenic hantaviruses replicate in the presence of high levels of MxA and other ISGs at late times post-infection remain to be investigated.

One report suggests that hantaviruses regulate IFN receptor directed STAT activation at later times post-infection. However, this data is inconsistent with the reported high level STAT-dependant induction of ISGs 2-4 days after hantavirus infection of endothelial cells. It is therefore unclear how ISGs are induced by hantaviruses if STAT-activation is regulated and this data is likely the misinterpretation of a STAT phosphorylation assay lacking proper controls (12, 28, 110). There are also conflicting reports suggesting that type-I interferons are not induced by hantaviruses, that early IFN responses are elicited by some

pathogenic hantaviruses or that inactivated hantaviruses induce early IFN responses (91, 92, 114). However, IFN transcription is transient and IFN ELISAs are of low sensitivity relative to assays of IFN function, which are amplified by IFN receptor directed ISG responses. Our lab and others have noted that IFN-β is induced by hantavirus infection of human endothelial cells and antibodies to IFN-β have previously been shown to enhance HTNV replication (37). Here we demonstrate that neutralizing antibodies to IFN-β inhibit the induction of ISGs following hantavirus infection and thus hantaviruse induced IFN-βsecretion directs ISG responses (82). Although reported, no explanation has been provided for how or why inactivated hantaviruses might play a role in inducing IFN responses in endothelial cells or the means by which this response might be elicited in an in vivo setting (40). Since virus is clearly sensitive to the induction or addition of IFN at early points post-infection it is also unclear how pathogenic hantaviruses might compensate for inactivated virus induction of early IFN responses.

Section 2: The Gn Cytoplasmic Tail Inhibits Interferon Induction by Disrupting TBK-TRAF3 complex formation.

We have determined that the Gn cytoplasmic tail from NY-1V inhibits TBK1 directed IFN-βsignaling pathways. Our findings show that the Gn cytoplasmic tail of the pathogenic NY-1V, but not PHV, suppresses ISRE and IFN-β promoter activation in response to RIG-I or TBK1 directed IFN pathway activation. These results indicate that the NY-1V Gn cytoplasmic tail inhibits IFN induction and functions in the regulation of IFN responses.

TBK1 and IKKε activate cytoplasmic forms of IRF-3 and NF-κB and activation permits their nuclear translocation and transcriptional responses. Activation of the IFN-β promoter is directed by an IRF-3, NF-κB, CBP/p300 transcription complex while ISRE promoters are activated by cellular IRFs but do not require NF-κB activation (31, 81). Our findings indicate that the Gn cytoplasmic tail inhibits both ISRE and IFN-β directed transcriptional responses consistent, with Gn inhibiting TBK1-IRF-3, and TBK directed NF-κB activation. However, the NY-1V Gn-tail had no effect on transcription directed by a constitutively active phospho-mimetic IRF-3 suggesting that Gn acts upstream of IRF-3 phosphorylation. Collectively our findings suggest that the Gn-tail functions to regulate IFN-β induction at the level of the TBK1 complex.

Previous studies have demonstrated that the NY-1V Gn cytoplasmic tail binds cellular Src and Syk family kinases and is ubiquitinated and degraded (26). Although it is unclear which proteins within the TBK1 complex are bound by Gn or whether Gn directs the degradation of specific TBK1 complex regulatory proteins, these possibilities provide plausible mechanisms for NY-1V Gn-tail regulation of TBK1 complex directed IFN signaling responses.

TBK1 forms a signaling complex with TRAF3, which links upstream signaling responses of IPS-1 (MAVs/Cardiff/VISA) to the TBK1 directed phosphorylation of IRF-3 and IFN-β transcriptional responses (77). IPS-1 binds to the C-terminal domain of TRAF3 (TRAF-C), while requirements for TRAF3 binding to TBK1 have yet to be determined (99). Our data indicates that the NY-1V Gn-tail binds to the TRAF3 N-terminus and the ability of the NY-1V Gn-tail to block TBK1-TRAF3 complex formation suggests that the Gn-tail either competes with TBK1 binding to TRAF3 or conformationally inhibits TBK1-TRAF3 interactions. TRAF3 forms trimers, an Gn-tail-TRAF interactions could also potentially disrupt TRAF3 oligomerization required for TBK1-TRAF3 binding.

Our findings further indicate that the NY-1V Gn-tail blocks NF-κB activation. In addition to TRAF3 directed IRF-3 phosphorylation, TBK1 directs NF-κB transcriptional responses by binding to TRAF2 (90). We have shown that the NY-1V Gn-tail regulates respective NF-κB and ISRE transcriptional

responses and binds the N-terminal domains of both TRAF2 and TRAF3 proteins. Instead of binding to TBK1, these findings suggest that the NY-1V Gn-tail binds a common N-terminal element within TRAF2 and TRAF3. These findings are consistent with reports that the N-terminal domains of TRAFs 3 and 5 are functionally interchangeable (34, 99). A cellular protein termed TNAP also reportedly binds TRAF3 and TRAF2 and represses NF-κB activation suggesting that the hantavirus Gn-tail may mimic a normal cellular IFN regulatory mechanism (43). The cellular protein A20 is a zinc finger containing protein with ubiquitin ligase activity, which also reportedly inhibits TBK1 directed IRF-3 and NF-κB activation (66, 122, 126). Interestingly, the NY-1V Gn-tail contains significant amino acid homology to both TNAP and A20, further suggesting that Gn may mimic the interferon regulatory capacities of these cellular proteins.

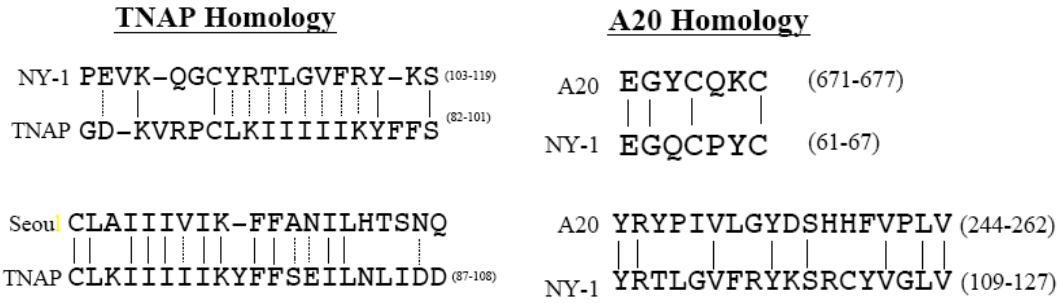

Figure 17. Amino acid alignments between sections of the NY-1V and Seoul virus Gn cytoplasmic tails and the cellular proteins TNAP and A20.

Since both IRF-3 activation and NF-κB activation are required to direct transcription from IFN promoters, this data suggests that Gn-tail regulation of IFN transcriptional responses may occur through the redundant inhibition of 2 required IFN signaling pathways. Data presented here further demonstrates that the Gn-tail of a pathogenic hantavirus inhibits pathway specific signaling responses that direct IFN transcription. Since both hantavirus infection and the Gn-tail block TBK1-TRAF3 complex formation these findings suggest a mechanism by which pathogenic hantaviruses inhibit early IFN transcriptional responses that might limit viral replication.

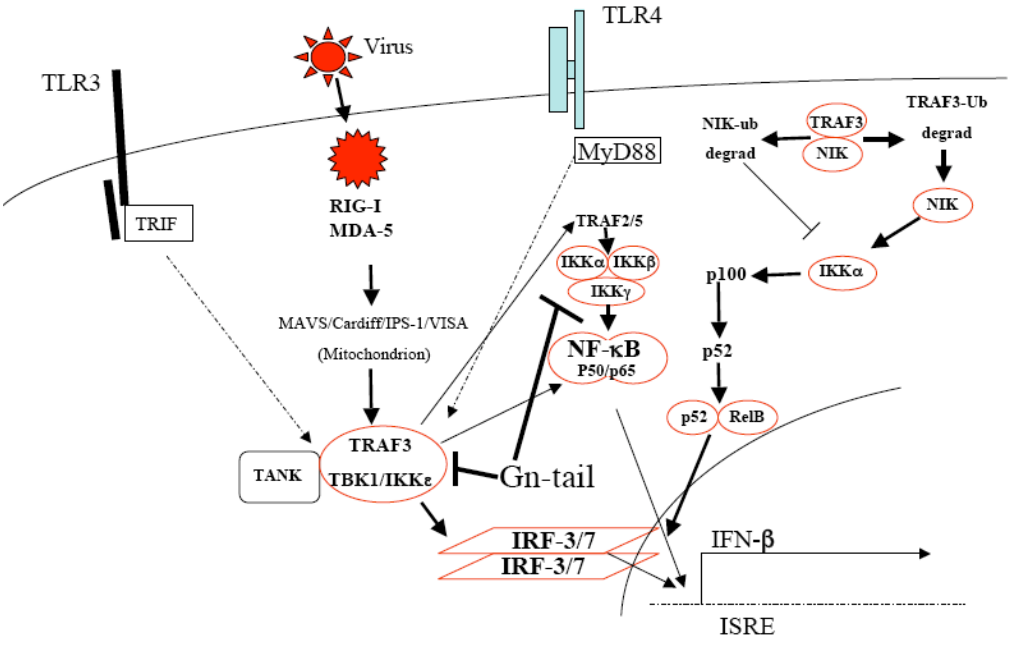

Figure 18. TRAF3 is at the Center of Responses that Direct NF-κB, ISRE and IFN Transcriptional Responses. The NY-1V Gn-tail binds TRAF3, disrupts TBK1-TRAF3 complex formation, and inhibits ISRE, IFN-β and NF-κB transcriptional responses

Hantaviruses express only 4 proteins and the Gn protein plays multiple roles in the hantavirus life cycle. The Gn protein is an envelope protein assembled into virions during budding into the cis-golgi. Gn forms heterodimeric complexes with Gc and the Gn cytoplasmic tail may also function as a matrix protein during the viral budding process (133). Although viral assembly clearly results in the accumulation of Gn into virions, the Gn-tail of pathogenic hantaviruses also contains a C-terminal degron which directs proteasomal degradation (106). It is unclear whether there is a switch in Gn stability that accounts for early Gn degradation and subsequent Gn accumulation following assembly. Interestingly, only pathogenic hantavirus Gn-tails are proteasomally degraded and further study is required to determine whether Gn-tail degradation contributes to the regulation of TBK1 complex formation and IFN transcriptional responses by pathogenic hantaviruses. TRAF3 is also linked to the proteasomal degradation pathway since TRAF3 interactions direct NF-κB inducing Kinase (NIK) degradation and suppress the non-canonical NF-κB activation pathway (34). It remains to be determined whether NY-1V Gn-tail interactions with TRAF3 are required for proteasomal degradation and whether the Gn-tail alters normal TRAF3 degradation responses, which could contribute to IFN regulation.

Viruses have evolved a variety of mechanisms to block IFN-β induction and antiviral immune responses. The Hepatitis C virus NS3/4A protein inhibits

RIG-I directed IFN-β induction by cleaving IPS-1 from the mitochondria while the VP35 protein of Ebola virus binds TBK1 and prevents IRF-3 directed IFN-β transcription (13, 19, 62, 64, 68, 75). The influenza virus NS1 protein is also an IFN antagonist with reported regulatory roles directed by dsRNA, RIG-I and IPS-1 binding interactions (7, 13, 30, 58, 75, 78). Although we have previously reported that the NY-1V Gn-tail also blocks TBK1 directed transcriptional responses, data presented here demonstrate that the Gn-tail binds TRAF3 which is required for TBK1 complexes to direct IRF-3 activation. The LMP1 protein of Epstein-Barr virus also binds TRAF3 through PxQxT motifs that reportedly regulate NF-κB activation although there is no information on whether these interactions regulate IFN responses (127). The NY-1V Gn-tail does not contain PxQxT motifs and as a result Gn-tail interactions with TRAF3 are discrete from those of LMP1. These findings suggest that the Gn-tail blocks IFN-β transcription through unique TRAF3 interactions. TRAF3 also forms trimeric structures with TRAF2, which are involved in NF-κB signaling (35). Disruption of TRAF3 and TRAF2 containing trimers is another possible mechanism the Gn-tail could use to regulate TBK1 directed innate immune responses.

Some members of the bunyavirdae family have been shown to encode a non-structural NSs protein, which inhibits IFN-β transcription 50 fold (8, 9, 125). Although NSs proteins have not previously been identified during HTNV, ANDV, SNV or NY-1V infection, a recent report suggests that Tula and Puumala

hantaviruses encode an NSs protein that reduces IFN-β transcription (45). However, Tula and Puumala NSs proteins inhibited IFN-β transcriptional responses by only 30% in data which lacks inadequate *Renilla* luciferase internal controls. As a result the contribution of these ORFs in IFN regulation is unclear (45). Additionally, corresponding NSs ORFs present in NY-1V, HTNV and ANDV are disrupted and this questions whether additional hantaviruses make an NSs protein. Although it is possible that hantaviruses have evolved redundant mechanisms for inhibiting IFN-β induction, the 40-50 fold reduction in IFN transcriptional responses directed by the NY-1V Gn-tail suggest that it plays a primary role in regulating early IFN responses during infection.

Collectively, our findings define an IFN pathway specific target bound by the pathogenic hantavirus Gn-tail. We demonstrate that the recombinant expressed NY-1V Gn-tail binds TRAF3 and disrupts TBK1-TRAF3 complex formation. Since pathogenic hantavirus infection of endothelial cells similarly disrupts TBK1-TRAF3 complex formation our findings suggest a mechanism for hantavirus regulation of IFN transcriptional responses that is directed by Gn-tail interactions with TRAF3. Collectively, our findings suggest that pathogenic hantaviruses disengage TBK1-TRAF3 complex formation at early times post-infection to prevent IFN-β induction.

Section 3: Future Directions

There are still many aspects of hantavirus directed regulation of the early cellular interferon response which remain unresolved. One of the major characteristics differentiating pathogenic hantavirus Gn-tails, from the Gn-tail of PHV, is the presence of a C-terminal degron which directs its proteasomal degradation. Whether proteasome mediated degradation is required for Gn-tail regulation of interferon signaling pathways remains unclear. Answering this question is an important step in fully understanding the mechanism of Gn-tail interferon inhibition since the TRAF3 binding studies presented here are done in the absence of a functional proteasome.

Further defining the Gn-TRAF3 binding interaction is also an important step in understanding how hantaviruses inhibit early interferon responses. Whether the Gn-tail competes for the TBK1 binding site, conformationally inhibits TBK1-TRAF3 binding, or targets TBK1 or TRAF3 for proteasomal degradation is currently unknown. All of these represent possible mechanisms of Gn-tail function and should be addressed. Finally, generation of a reverse genetics system for hantavirus would allow for the in vivo analysis of Gn-tail effects on interferon responses.

References

1. **Aebi, M., J. Fah, N. Hurt, C. E. Samuel, D. Thomis, L. Bazzigher, J. Pavlovic, O. Haller, and P. Staeheli.** 1989. cDNA structures and regulation of two interferon-induced human Mx proteins. Mol Cell Biol **9:**5062-72.
2. **Alcami, A., J. A. Symons, and G. L. Smith.** 2000. The vaccinia virus soluble alpha/beta interferon (IFN) receptor binds to the cell surface and protects cells from the antiviral effects of IFN. J Virol **74:**11230-9.
3. **Alff, P. J., I. N. Gavrilovskaya, E. Gorbunova, K. Endriss, Y. Chong, E. Geimonen, N. Sen, N. C. Reich, and E. R. Mackow.** 2006. The pathogenic NY-1 hantavirus G1 cytoplasmic tail inhibits RIG-I- and TBK1-directed interferon responses. J Virol **80:**9676-86.
4. **Bai, J., K. Zhu, and G. Zhou.** 1997. [The therapeutic effect of purified human leucocytic interferon-alpha on hemorrhagic fever with renal syndrome]. Zhonghua Nei Ke Za Zhi **36:**90-3.
5. **Barro, M., and J. T. Patton.** 2005. Rotavirus nonstructural protein 1 subverts innate immune response by inducing degradation of IFN regulatory factor 3. Proc Natl Acad Sci U S A **102:**4114-9.
6. **Basler, C. F., and A. Garcia-Sastre.** 2002. Viruses and the type I interferon antiviral system: induction and evasion. Int Rev Immunol **21:**305-37.

7. **Basler, C. F., A. Mikulasova, L. Martinez-Sobrido, J. Paragas, E. Muhlberger, M. Bray, H. D. Klenk, P. Palese, and A. Garcia-Sastre.** 2003. The Ebola virus VP35 protein inhibits activation of interferon regulatory factor 3. J Virol **77:**7945-56.

8. **Billecocq, A., M. Spiegel, P. Vialat, A. Kohl, F. Weber, M. Bouloy, and O. Haller.** 2004. NSs protein of Rift Valley fever virus blocks interferon production by inhibiting host gene transcription. J Virol **78:**9798-806.

9. **Blakqori, G., S. Delhaye, M. Habjan, C. D. Blair, I. Sanchez-Vargas, K. E. Olson, G. Attarzadeh-Yazdi, R. Fragkoudis, A. Kohl, U. Kalinke, S. Weiss, T. Michiels, P. Staeheli, and F. Weber.** 2007. La Crosse bunyavirus nonstructural protein NSs serves to suppress the type I interferon system of mammalian hosts. J Virol **81:**4991-9.

10. **Bren, A. F., S. K. Pavlovcic, M. Koselj, J. Kovac, A. Kandus, and R. Kveder.** 1996. Acute renal failure due to hemorrhagic fever with renal syndrome. Ren Fail **18:**635-8.

11. **Brierley, M. M., and E. N. Fish.** 2002. Review: IFN-alpha/beta receptor interactions to biologic outcomes: understanding the circuitry. J Interferon Cytokine Res **22:**835-45.

12. **Brierley, M. M., and E. N. Fish.** 2005. Stats: multifaceted regulators of transcription. J Interferon Cytokine Res **25:**733-44.

13. **Cardenas, W. B., Y. M. Loo, M. Gale, Jr., A. L. Hartman, C. R. Kimberlin, L. Martinez-Sobrido, E. O. Saphire, and C. F. Basler.** 2006. Ebola virus VP35 protein binds double-stranded RNA and inhibits alpha/beta interferon production induced by RIG-I signaling. J Virol **80:**5168-78.

14. **Cosgriff, T. M.** 1991. Mechanisms of disease in Hantavirus infection: pathophysiology of hemorrhagic fever with renal syndrome. Rev Infect Dis **13:**97-107.

15. **Emeny, J. M., and M. J. Morgan.** 1979. Regulation of the interferon system: evidence that Vero cells have a genetic defect in interferon production. J Gen Virol **43:**247-52.

16. **Espinoza, R., P. Vial, L. M. Noriega, A. Johnson, S. T. Nichol, P. E. Rollin, R. Wells, S. Zaki, E. Reynolds, and T. G. Ksiazek.** 1998. Hantavirus pulmonary syndrome in a Chilean patient with recent travel in Bolivia. Emerg Infect Dis **4:**93-5.

17. **Evans, J. D., and C. Seeger.** 2006. Cardif: a protein central to innate immunity is inactivated by the HCV NS3 serine protease. Hepatology **43:**615-7.

18. **Ferres, M., P. Vial, C. Marco, L. Yanez, P. Godoy, C. Castillo, B. Hjelle, I. Delgado, S. J. Lee, and G. J. Mertz.** 2007. Prospective

evaluation of household contacts of persons with hantavirus cardiopulmonary syndrome in chile. J Infect Dis **195:**1563-71.

19. **Foy, E., K. Li, C. Wang, R. Sumpter, Jr., M. Ikeda, S. M. Lemon, and M. Gale, Jr.** 2003. Regulation of interferon regulatory factor-3 by the hepatitis C virus serine protease. Science **300:**1145-8.

20. **Frese, M., G. Kochs, H. Feldmann, C. Hertkorn, and O. Haller.** 1996. Inhibition of bunyaviruses, phleboviruses, and hantaviruses by human MxA protein. J Virol **70:**915-23.

21. **Fujita, T., K. Onoguchi, K. Onomoto, R. Hirai, and M. Yoneyama.** 2007. Triggering antiviral response by RIG-I-related RNA helicases. Biochimie **89:**754-60.

22. **Garcia-Sastre, A., and C. A. Biron.** 2006. Type 1 interferons and the virus-host relationship: a lesson in detente. Science **312:**879-82.

23. **Gavrilovskaya, I., R. LaMonica, M. E. Fay, B. Hjelle, C. Schmaljohn, R. Shaw, and E. R. Mackow.** 1999. New York 1 and Sin Nombre viruses are serotypically distinct viruses associated with hantavirus pulmonary syndrome. J Clin Microbiol **37:**122-6.

24. **Gavrilovskaya, I. N., E. J. Brown, M. H. Ginsberg, and E. R. Mackow.** 1999. Cellular entry of hantaviruses which cause hemorrhagic fever with renal syndrome is mediated by beta3 integrins. J Virol **73:**3951-9.

25. **Gavrilovskaya, I. N., M. Shepley, R. Shaw, M. H. Ginsberg, and E. R. Mackow.** 1998. beta3 Integrins mediate the cellular entry of hantaviruses that cause respiratory failure. Proc Natl Acad Sci U S A **95:**7074-9.

26. **Geimonen, E., I. Fernandez, I. N. Gavrilovskaya, and E. R. Mackow.** 2003. Tyrosine residues direct the ubiquitination and degradation of the NY-1 hantavirus G1 cytoplasmic tail. J Virol **77:**10760-868.

27. **Geimonen, E., R. LaMonica, K. Springer, Y. Farooqui, I. N. Gavrilovskaya, and E. R. Mackow.** 2003. Hantavirus pulmonary syndrome-associated hantaviruses contain conserved and functional ITAM signaling elements. J Virol **77:**1638-43.

28. **Geimonen, E., S. Neff, T. Raymond, S. S. Kocer, I. N. Gavrilovskaya, and E. R. Mackow.** 2002. Pathogenic and nonpathogenic hantaviruses differentially regulate endothelial cell responses. Proc Natl Acad Sci U S A **99:**13837-42.

29. **Graff, J. W., J. Ewen, K. Ettayebi, and M. E. Hardy.** 2007. Zinc-binding domain of rotavirus NSP1 is required for proteasome-dependent degradation of IRF3 and autoregulatory NSP1 stability. J Gen Virol **88:**613-20.

30. **Guo, Z., L. M. Chen, H. Zeng, J. A. Gomez, J. Plowden, T. Fujita, J. M. Katz, R. O. Donis, and S. Sambhara.** 2007. NS1 protein of influenza

A virus inhibits the function of intracytoplasmic pathogen sensor, RIG-I. Am J Respir Cell Mol Biol **36:**263-9.

31. **Hacker, H., and M. Karin.** 2006. Regulation and function of IKK and IKK-related kinases. Sci STKE **2006:**re13.

32. **Hacker, H., V. Redecke, B. Blagoev, I. Kratchmarova, L. C. Hsu, G. G. Wang, M. P. Kamps, E. Raz, H. Wagner, G. Hacker, M. Mann, and M. Karin.** 2006. Specificity in Toll-like receptor signalling through distinct effector functions of TRAF3 and TRAF6. Nature **439:**204-7.

33. **Haller, O., M. Frese, and G. Kochs.** 1998. Mx proteins: mediators of innate resistance to RNA viruses. Rev Sci Tech **17:**220-30.

34. **He, J. Q., S. K. Saha, J. R. Kang, B. Zarnegar, and G. Cheng.** 2007. Specificity of TRAF3 in its negative regulation of the noncanonical NF-kappa B pathway. J Biol Chem **282:**3688-94.

35. **He, L., A. C. Grammer, X. Wu, and P. E. Lipsky.** 2004. TRAF3 forms heterotrimers with TRAF2 and modulates its ability to mediate NF-{kappa}B activation. J Biol Chem **279:**55855-65.

36. **Henderson, W. W., M. C. Monroe, S. C. St Jeor, W. P. Thayer, J. E. Rowe, C. J. Peters, and S. T. Nichol.** 1995. Naturally occurring Sin Nombre virus genetic reassortants. Virology **214:**602-10.

37. **Hengel, H., U. H. Koszinowski, and K. K. Conzelmann.** 2005. Viruses know it all: new insights into IFN networks. Trends Immunol **26:**396-401.

38. **Hiscott, J.** 2007. Triggering the innate antiviral response through IRF-3 activation. J Biol Chem **282:**15325-9.

39. **Hiscott, J., N. Grandvaux, S. Sharma, B. R. Tenoever, M. J. Servant, and R. Lin.** 2003. Convergence of the NF-kappaB and interferon signaling pathways in the regulation of antiviral defense and apoptosis. Ann N Y Acad Sci **1010:**237-48.

40. **Hiscott, J., J. Lacoste, and R. Lin.** 2006. Recruitment of an interferon molecular signaling complex to the mitochondrial membrane: disruption by hepatitis C virus NS3-4A protease. Biochem Pharmacol **72:**1477-84.

41. **Hiscott, J., R. Lin, P. Nakhaei, and S. Paz.** 2006. MasterCARD: a priceless link to innate immunity. Trends Mol Med **12:**53-6.

42. **Hooper, J. W., T. Larsen, D. M. Custer, and C. S. Schmaljohn.** 2001. A lethal disease model for hantavirus pulmonary syndrome. Virology **289:**6-14.

43. **Hu, W. H., X. M. Mo, W. M. Walters, R. Brambilla, and J. R. Bethea.** 2004. TNAP, a novel repressor of NF-kappaB-inducing kinase, suppresses NF-kappaB activation. J Biol Chem **279:**35975-83.

44. **Hughes, J. M., C. J. Peters, M. L. Cohen, and B. W. Mahy.** 1993. Hantavirus pulmonary syndrome: an emerging infectious disease [see comments]. Science **262:**850-1.

45. **Jaaskelainen, K. M., P. Kaukinen, E. S. Minskaya, A. Plyusnina, O. Vapalahti, R. M. Elliott, F. Weber, A. Vaheri, and A. Plyusnin.** 2007. Tula and Puumala hantavirus NSs ORFs are functional and the products inhibit activation of the interferon-beta promoter. J Med Virol **79:**1527-36.

46. **Johnson, A. M., M. D. Bowen, T. G. Ksiazek, R. J. Williams, R. T. Bryan, J. N. Mills, C. J. Peters, and S. T. Nichol.** 1997. Laguna Negra virus associated with HPS in western Paraguay and Bolivia. Virology **238:**115-27.

47. **Johnson, A. M., L. T. de Souza, I. B. Ferreira, L. E. Pereira, T. G. Ksiazek, P. E. Rollin, C. J. Peters, and S. T. Nichol.** 1999. Genetic investigation of novel hantaviruses causing fatal HPS in Brazil. J Med Virol **59:**527-35.

48. **Johnson, K. M.** 2001. Hantaviruses: history and overview. Curr Top Microbiol Immunol **256:**1-14.

49. **Kanerva, M., K. Melen, A. Vaheri, and I. Julkunen.** 1996. Inhibition of puumala and tula hantaviruses in Vero cells by MxA protein. Virology **224:**55-62.

50. **Kato, H., O. Takeuchi, S. Sato, M. Yoneyama, M. Yamamoto, K. Matsui, S. Uematsu, A. Jung, T. Kawai, K. J. Ishii, O. Yamaguchi, K. Otsu, T. Tsujimura, C. S. Koh, C. Reis e Sousa, Y. Matsuura, T.**

Fujita, and S. Akira. 2006. Differential roles of MDA5 and RIG-I helicases in the recognition of RNA viruses. Nature **441:**101-5.

51. **Kawai, T., and S. Akira.** 2007. Antiviral signaling through pattern recognition receptors. J Biochem (Tokyo) **141:**137-45.

52. **Kawai, T., K. Takahashi, S. Sato, C. Coban, H. Kumar, H. Kato, K. J. Ishii, O. Takeuchi, and S. Akira.** 2005. IPS-1, an adaptor triggering RIG-I- and Mda5-mediated type I interferon induction. Nat Immunol **6:**981-8.

53. **Khan, A., and A. S. Khan.** 2003. Hantaviruses: a tale of two hemispheres. Panminerva Med **45:**43-51.

54. **Khan, A. S., P. T. Kitsutani, and A. L. Corneli.** 2000. Hantavirus pulmonary syndrome in the Americas: the early years. Semin Respir Crit Care Med **21:**313-22.

55. **Khan, A. S., and J. C. Young.** 2001. Hantavirus pulmonary syndrome: at the crossroads. Curr Opin Infect Dis **14:**205-9.

56. **Kim, Y. K., S. C. Lee, C. Kim, S. T. Heo, C. Choi, and J. M. Kim.** 2007. Clinical and laboratory predictors of oliguric renal failure in haemorrhagic fever with renal syndrome caused by Hantaan virus. J Infect **54:**381-6.

57. **Kitsutani, P. T., R. W. Denton, C. L. Fritz, R. A. Murray, R. L. Todd, W. J. Pape, J. Wyatt Frampton, J. C. Young, A. S. Khan, C. J. Peters,**

and T. G. Ksiazek. 1999. Acute Sin Nombre hantavirus infection without pulmonary syndrome, United States. Emerg Infect Dis **5:**701-5.

58. **Kochs, G., A. Garcia-Sastre, and L. Martinez-Sobrido.** 2007. Multiple anti-interferon actions of the influenza A virus NS1 protein. J Virol **81:**7011-21.

59. **Kraus, A. A., M. J. Raftery, T. Giese, R. Ulrich, R. Zawatzky, S. Hippenstiel, N. Suttorp, D. H. Kruger, and G. Schonrich.** 2004. Differential antiviral response of endothelial cells after infection with pathogenic and nonpathogenic hantaviruses. J Virol **78:**6143-50.

60. **Lee, H. W., and G. van der Groen.** 1989. Hemorrhagic fever with renal syndrome. Prog Med Virol **36:**62-102.

61. **Lee, M. S., and Y. J. Kim.** 2007. Pattern-recognition receptor signaling initiated from extracellular, membrane, and cytoplasmic space. Mol Cells **23:**1-10.

62. **Li, X. D., L. Sun, R. B. Seth, G. Pineda, and Z. J. Chen.** 2005. Hepatitis C virus protease NS3/4A cleaves mitochondrial antiviral signaling protein off the mitochondria to evade innate immunity. Proc Natl Acad Sci U S A **102:**17717-22.

63. **Lin, R., C. Heylbroeck, P. Genin, P. M. Pitha, and J. Hiscott.** 1999. Essential role of interferon regulatory factor 3 in direct activation of RANTES chemokine transcription. Mol Cell Biol **19:**959-66.

64. **Lin, R., J. Lacoste, P. Nakhaei, Q. Sun, L. Yang, S. Paz, P. Wilkinson, I. Julkunen, D. Vitour, E. Meurs, and J. Hiscott.** 2006. Dissociation of a MAVS/IPS-1/VISA/Cardif-IKKepsilon molecular complex from the mitochondrial outer membrane by hepatitis C virus NS3-4A proteolytic cleavage. J Virol **80:**6072-83.

65. **Lin, R., Y. Mamane, and J. Hiscott.** 1999. Structural and functional analysis of interferon regulatory factor 3: localization of the transactivation and autoinhibitory domains. Mol Cell Biol **19:**2465-74.

66. **Lin, R., L. Yang, P. Nakhaei, Q. Sun, E. Sharif-Askari, I. Julkunen, and J. Hiscott.** 2006. Negative regulation of the retinoic acid-inducible gene I-induced antiviral state by the ubiquitin-editing protein A20. J Biol Chem **281:**2095-103.

67. **Lober, C., B. Anheier, S. Lindow, H. D. Klenk, and H. Feldmann.** 2001. The Hantaan virus glycoprotein precursor is cleaved at the conserved pentapeptide WAASA. Virology **289:**224-9.

68. **Loo, Y. M., D. M. Owen, K. Li, A. K. Erickson, C. L. Johnson, P. M. Fish, D. S. Carney, T. Wang, H. Ishida, M. Yoneyama, T. Fujita, T. Saito, W. M. Lee, C. H. Hagedorn, D. T. Lau, S. A. Weinman, S. M. Lemon, and M. Gale, Jr.** 2006. Viral and therapeutic control of IFN-beta promoter stimulator 1 during hepatitis C virus infection. Proc Natl Acad Sci U S A **103:**6001-6.

69. **Lyubsky, S., I. Gavrilovskaya, B. Luft, and E. Mackow.** 1996. Histopathology of Peromyscus leucopus naturally infected with pathogenic NY-1 hantaviruses: pathologic markers of HPS viral infection in mice. Lab Invest **74:**627-33.

70. **Mackow, E. R., B. J. Luft, E. Bosler, and D. Goldgaber.** 1995. More on hantavirus in New England and New York. N Engl J Med **332:**337-8.

71. **Medhurst, A. D., D. C. Harrison, S. J. Read, C. A. Campbell, M. J. Robbins, and M. N. Pangalos.** 2000. The use of TaqMan RT-PCR assays for semiquantitative analysis of gene expression in CNS tissues and disease models. J Neurosci Methods **98:**9-20.

72. **Medina, R. A., K. Mirowsky-Garcia, J. Hutt, and B. Hjelle.** 2007. Ribavirin, human convalescent plasma and anti-beta3 integrin antibody inhibit infection by Sin Nombre virus in the deer mouse model. J Gen Virol **88:**493-505.

73. **Mertz, G. J., L. Miedzinski, D. Goade, A. T. Pavia, B. Hjelle, C. O. Hansbarger, H. Levy, F. T. Koster, K. Baum, A. Lindemulder, W. Wang, L. Riser, H. Fernandez, and R. J. Whitley.** 2004. Placebo-controlled, double-blind trial of intravenous ribavirin for the treatment of hantavirus cardiopulmonary syndrome in North America. Clin Infect Dis **39:**1307-13.

74. **Meylan, E., J. Curran, K. Hofmann, D. Moradpour, M. Binder, R. Bartenschlager, and J. Tschopp.** 2005. Cardif is an adaptor protein in the RIG-I antiviral pathway and is targeted by hepatitis C virus. Nature **437:**1167-72.

75. **Mibayashi, M., L. Martinez-Sobrido, Y. M. Loo, W. B. Cardenas, M. Gale, Jr., and A. Garcia-Sastre.** 2007. Inhibition of retinoic acid-inducible gene I-mediated induction of beta interferon by the NS1 protein of influenza A virus. J Virol **81:**514-24.

76. **Noppert, S. J., K. A. Fitzgerald, and P. J. Hertzog.** 2007. The role of type I interferons in TLR responses. Immunol Cell Biol.

77. **Oganesyan, G., S. K. Saha, B. Guo, J. Q. He, A. Shahangian, B. Zarnegar, A. Perry, and G. Cheng.** 2006. Critical role of TRAF3 in the Toll-like receptor-dependent and -independent antiviral response. Nature **439:**208-11.

78. **Opitz, B., A. Rejaibi, B. Dauber, J. Eckhard, M. Vinzing, B. Schmeck, S. Hippenstiel, N. Suttorp, and T. Wolff.** 2007. IFNbeta induction by influenza A virus is mediated by RIG-I which is regulated by the viral NS1 protein. Cell Microbiol **9:**930-8.

79. **Overby, A. K., V. L. Popov, R. F. Pettersson, and E. P. Neve.** 2007. The cytoplasmic tails of Uukuniemi virus (Bunyaviridae) GN and GC

glycoproteins are important for intracellular targeting and the budding of VLPs. J Virol.

80. **Paladino, P., D. T. Cummings, R. S. Noyce, and K. L. Mossman.** 2006. The IFN-independent response to virus particle entry provides a first line of antiviral defense that is independent of TLRs and retinoic acid-inducible gene I. J Immunol **177:**8008-16.

81. **Paz, S., Q. Sun, P. Nakhaei, R. Romieu-Mourez, D. Goubau, I. Julkunen, R. Lin, and J. Hiscott.** 2006. Induction of IRF-3 and IRF-7 phosphorylation following activation of the RIG-I pathway. Cell Mol Biol (Noisy-le-grand) **52:**17-28.

82. **Pensiero, M. N., J. B. Sharefkin, C. W. Dieffenbach, and J. Hay.** 1992. Hantaan virus infection of human endothelial cells. J Virol **66:**5929-36.

83. **Peters, C. J., and A. S. Khan.** 2002. Hantavirus pulmonary syndrome: the new American hemorrhagic fever. Clin Infect Dis **34:**1224-31.

84. **Peters, C. J., G. L. Simpson, and H. Levy.** 1999. Spectrum of hantavirus infection: hemorrhagic fever with renal syndrome and hantavirus pulmonary syndrome. Annu Rev Med **50:**531-45.

85. **Pichlmair, A., O. Schulz, C. P. Tan, T. I. Naslund, P. Liljestrom, F. Weber, and C. Reis e Sousa.** 2006. RIG-I-mediated antiviral responses to single-stranded RNA bearing 5'-phosphates. Science **314:**997-1001.

86. **Pietila, T. E., V. Veckman, A. Lehtonen, R. Lin, J. Hiscott, and I. Julkunen.** 2007. Multiple NF-kappaB and IFN regulatory factor family transcription factors regulate CCL19 gene expression in human monocyte-derived dendritic cells. J Immunol **178:**253-61.

87. **Pietras, E. M., S. K. Saha, and G. Cheng.** 2006. The interferon response to bacterial and viral infections. J Endotoxin Res **12:**246-50.

88. **Pini, N., S. Levis, G. Calderon, J. Ramirez, D. Bravo, E. Lozano, C. Ripoll, S. St Jeor, T. G. Ksiazek, R. M. Barquez, and D. Enria.** 2003. Hantavirus infection in humans and rodents, northwestern Argentina. Emerg Infect Dis **9:**1070-6.

89. **Plyusnin, A., O. Vapalahti, and A. Vaheri.** 1996. Hantaviruses: genome structure, expression and evolution. J Gen Virol **77 (Pt 11):**2677-87.

90. **Pomerantz, J. L., and D. Baltimore.** 1999. NF-kappaB activation by a signaling complex containing TRAF2, TANK and TBK1, a novel IKK-related kinase. Embo J **18:**6694-704.

91. **Prescott, J., C. Ye, G. Sen, and B. Hjelle.** 2005. Induction of innate immune response genes by Sin Nombre hantavirus does not require viral replication. J Virol **79:**15007-15.

92. **Prescott, J. B., P. R. Hall, V. S. Bondu-Hawkins, C. Ye, and B. Hjelle.** 2007. Early innate immune responses to Sin Nombre hantavirus occur

independently of IFN regulatory factor 3, characterized pattern recognition receptors, and viral entry. J Immunol **179:**1796-802.

93. **Ravkov, E. V., S. T. Nichol, and R. W. Compans.** 1997. Polarized entry and release in epithelial cells of Black Creek Canal virus, a New World hantavirus. J Virol **71:**1147-54.

94. **Reich, N. C.** 2002. Nuclear/cytoplasmic localization of IRFs in response to viral infection or interferon stimulation. J Interferon Cytokine Res **22:**103-9.

95. **Riquelme, R., M. Riquelme, A. Torres, M. L. Rioseco, J. A. Vergara, L. Scholz, and A. Carriel.** 2003. Hantavirus pulmonary syndrome, southern Chile. Emerg Infect Dis **9:**1438-43.

96. **Rizvanov, A. A., S. F. Khaiboullina, and S. St Jeor.** 2004. Development of reassortant viruses between pathogenic hantavirus strains. Virology **327:**225-32.

97. **Rodriguez, L. L., J. H. Owens, C. J. Peters, and S. T. Nichol.** 1998. Genetic reassortment among viruses causing hantavirus pulmonary syndrome. Virology **242:**99-106.

98. **Rothe, M., V. Sarma, V. M. Dixit, and D. V. Goeddel.** 1995. TRAF2-mediated activation of NF-kappa B by TNF receptor 2 and CD40. Science **269:**1424-7.

99. **Saha, S. K., E. M. Pietras, J. Q. He, J. R. Kang, S. Y. Liu, G. Oganesyan, A. Shahangian, B. Zarnegar, T. L. Shiba, Y. Wang, and G. Cheng.** 2006. Regulation of antiviral responses by a direct and specific interaction between TRAF3 and Cardif. Embo J **25:**3257-63.

100. **Saito, T., and M. Gale, Jr.** 2007. Principles of intracellular viral recognition. Curr Opin Immunol **19:**17-23.

101. **Samuel, C. E.** 2001. Antiviral actions of interferons. Clin Microbiol Rev **14:**778-809, table of contents.

102. **Schmaljohn, C., and B. F. (ed.).** 2001. Bunyaviridae and their Replication. Fields Virology 4th edition **1:**p. 1581-1602.

103. **Schmaljohn, C., and B. Hjelle.** 1997. Hantaviruses: a global disease problem. Emerg Infect Dis **3:**95-104.

104. **Schmaljohn, C. S., G. B. Jennings, J. Hay, and J. M. Dalrymple.** 1986. Coding strategy of the S genome segment of Hantaan virus. Virology **155:**633-43.

105. **Schmaljohn, C. S., A. L. Schmaljohn, and J. M. Dalrymple.** 1987. Hantaan virus M RNA: coding strategy, nucleotide sequence, and gene order. Virology **157:**31-9.

106. **Sen, N., A. Sen, and E. R. Mackow.** 2007. Degrons at the C terminus of the pathogenic but not the nonpathogenic hantavirus G1 tail direct proteasomal degradation. J Virol **81:**4323-30.

107. **Seth, R. B., L. Sun, C. K. Ea, and Z. J. Chen.** 2005. Identification and characterization of MAVS, a mitochondrial antiviral signaling protein that activates NF-kappaB and IRF 3. Cell **122:**669-82.

108. **Shi, X., and R. M. Elliott.** 2002. Golgi localization of Hantaan virus glycoproteins requires coexpression of G1 and G2. Virology **300:**31-8.

109. **Song, J., B. L., I. Gavrilovskaya, E. Mackow, B. Hjelle, and R. _. Yanigahara.** 1996. Sequence analysis of the complete S genomic segment of a newly identified hantavirus isolated from the white footed mouse (P. leucopus): Phylogenetic relationship with other Sigmadontine rodent borne hantaviruses. Virus Genes **12:**249-256.

110. **Spiropoulou, C. F.** 2001. Hantavirus maturation. Curr Top Microbiol Immunol **256:**33-46.

111. **Spiropoulou, C. F., S. Morzunov, H. Feldmann, A. Sanchez, C. J. Peters, and S. T. Nichol.** 1994. Genome structure and variability of a virus causing hantavirus pulmonary syndrome. Virology **200:**715-23.

112. **Stephen, C., M. Johnson, and A. Bell.** 1994. First reported cases of hantavirus pulmonary syndrome in Canada. Can Commun Dis Rep **20:**121-5.

113. **Sumpter, R., Jr., Y. M. Loo, E. Foy, K. Li, M. Yoneyama, T. Fujita, S. M. Lemon, and M. Gale, Jr.** 2005. Regulating intracellular antiviral

defense and permissiveness to hepatitis C virus RNA replication through a cellular RNA helicase, RIG-I. J Virol **79:**2689-99.

114. **Sundstrom, J. B., L. K. McMullan, C. F. Spiropoulou, W. C. Hooper, A. A. Ansari, C. J. Peters, and P. E. Rollin.** 2001. Hantavirus infection induces the expression of RANTES and IP-10 without causing increased permeability in human lung microvascular endothelial cells. J Virol **75:**6070-85.

115. **Symons, J. A., A. Alcami, and G. L. Smith.** 1995. Vaccinia virus encodes a soluble type I interferon receptor of novel structure and broad species specificity. Cell **81:**551-60.

116. **Tai, P. W., L. C. Chen, and C. H. Huang.** 2005. Hanta hemorrhagic fever with renal syndrome: a case report and review. J Microbiol Immunol Infect **38:**221-3.

117. **Tamura, M., H. Asada, K. Kondo, M. Takahashi, and K. Yamanishi.** 1987. Effects of human and murine interferons against hemorrhagic fever with renal syndrome (HFRS) virus (Hantaan virus). Antiviral Res **8:**171-8.

118. **Temonen, M., H. Lankinen, O. Vapalahti, T. Ronni, I. Julkunen, and A. Vaheri.** 1995. Effect of interferon-alpha and cell differentiation on Puumala virus infection in human monocyte/macrophages. Virology **206:**8-15.

119. **Thompson, A. J., and S. A. Locarnini.** 2007. Toll-like receptors, RIG-I-like RNA helicases and the antiviral innate immune response. Immunol Cell Biol.

120. **Vapalahti, O., A. Lundkvist, S. K. Kukkonen, Y. Cheng, M. Gilljam, M. Kanerva, T. Manni, M. Pejcoch, J. Niemimaa, A. Kaikusalo, H. Henttonen, A. Vaheri, and A. Plyusnin.** 1996. Isolation and characterization of Tula virus, a distinct serotype in the genus Hantavirus, family Bunyaviridae. J Gen Virol **77 (Pt 12):**3063-7.

121. **Verma, A., S. Kambhampati, S. Parmar, and L. C. Platanias.** 2003. Jak family of kinases in cancer. Cancer Metastasis Rev **22:**423-34.

122. **Wang, Y. Y., L. Li, K. J. Han, Z. Zhai, and H. B. Shu.** 2004. A20 is a potent inhibitor of TLR3- and Sendai virus-induced activation of NF-kappaB and ISRE and IFN-beta promoter. FEBS Lett **576:**86-90.

123. **Wathelet, M. G., P. M. Berr, and G. A. Huez.** 1992. Regulation of gene expression by cytokines and virus in human cells lacking the type-I interferon locus. Eur J Biochem **206:**901-10.

124. **Weaver, B. K., K. P. Kumar, and N. C. Reich.** 1998. Interferon regulatory factor 3 and CREB-binding protein/p300 are subunits of double-stranded RNA-activated transcription factor DRAF1. Mol Cell Biol **18:**1359-68.

125. **Weber, F., A. Bridgen, J. K. Fazakerley, H. Streitenfeld, N. Kessler, R. E. Randall, and R. M. Elliott.** 2002. Bunyamwera bunyavirus nonstructural protein NSs counteracts the induction of alpha/beta interferon. J Virol **76:**7949-55.

126. **Wertz, I. E., K. M. O'Rourke, H. Zhou, M. Eby, L. Aravind, S. Seshagiri, P. Wu, C. Wiesmann, R. Baker, D. L. Boone, A. Ma, E. V. Koonin, and V. M. Dixit.** 2004. De-ubiquitination and ubiquitin ligase domains of A20 downregulate NF-kappaB signalling. Nature **430:**694-9.

127. **Wu, S., P. Xie, K. Welsh, C. Li, C. Z. Ni, X. Zhu, J. C. Reed, A. C. Satterthwait, G. A. Bishop, and K. R. Ely.** 2005. LMP1 protein from the Epstein-Barr virus is a structural CD40 decoy in B lymphocytes for binding to TRAF3. J Biol Chem **280:**33620-6.

128. **Xu, L. G., Y. Y. Wang, K. J. Han, L. Y. Li, Z. Zhai, and H. B. Shu.** 2005. VISA is an adapter protein required for virus-triggered IFN-beta signaling. Mol Cell **19:**727-40.

129. **Yanagihara, R., C. A. Daum, P. W. Lee, L. J. Baek, H. L. Amyx, D. C. Gajdusek, and C. J. Gibbs.** 1987. Serological survey of Prospect Hill virus infection in indigenous wild rodents in the USA. Trans R Soc Trop Med Hyg **81:**42-5.

130. **Yanagihara, R., and D. J. Silverman.** 1990. Experimental infection of human vascular endothelial cells by pathogenic and nonpathogenic hantaviruses. Arch Virol **111:**281-6.

131. **Yoneyama, M., M. Kikuchi, T. Natsukawa, N. Shinobu, T. Imaizumi, M. Miyagishi, K. Taira, S. Akira, and T. Fujita.** 2004. The RNA helicase RIG-I has an essential function in double-stranded RNA-induced innate antiviral responses. Nat Immunol **5:**730-7.

132. **Young, J. C., G. R. Hansen, T. K. Graves, M. P. Deasy, J. G. Humphreys, C. L. Fritz, K. L. Gorham, A. S. Khan, T. G. Ksiazek, K. B. Metzger, and C. J. Peters.** 2000. The incubation period of hantavirus pulmonary syndrome. Am J Trop Med Hyg **62:**714-7.

133. **Zaki, S. R., P. W. Greer, L. M. Coffield, C. S. Goldsmith, K. B. Nolte, K. Foucar, R. M. Feddersen, R. E. Zumwalt, G. L. Miller, A. S. Khan, and et al.** 1995. Hantavirus pulmonary syndrome. Pathogenesis of an emerging infectious disease. Am J Pathol **146:**552-79.

134. **Zhou, Z., O. J. Hamming, N. Ank, S. R. Paludan, A. L. Nielsen, and R. Hartmann.** 2007. Type III interferon (IFN) induces a type I IFN-like response in a restricted subset of cells through signaling pathways involving both the Jak-STAT pathway and the mitogen-activated protein kinases. J Virol **81:**7749-58.